



HAL
open science

Spectroscopy of B-type asteroids: Subgroups and meteorite analogs

Beth E. Clark, Julie Ziffer, David Nesvorny, Humberto Campins, Andrew S. Rivkin, Takahiro Hiroi, Maria Antonella Barucci, Marcello Fulchignoni, Richard P. Binzel, Sonia Fornasier, et al.

► **To cite this version:**

Beth E. Clark, Julie Ziffer, David Nesvorny, Humberto Campins, Andrew S. Rivkin, et al.. Spectroscopy of B-type asteroids: Subgroups and meteorite analogs. *Journal of Geophysical Research. Planets*, 2010, 115, pp.06005. 10.1029/2009JE003478 . hal-03730884

HAL Id: hal-03730884

<https://hal.science/hal-03730884>

Submitted on 7 Sep 2022

HAL is a multi-disciplinary open access archive for the deposit and dissemination of scientific research documents, whether they are published or not. The documents may come from teaching and research institutions in France or abroad, or from public or private research centers.

L'archive ouverte pluridisciplinaire **HAL**, est destinée au dépôt et à la diffusion de documents scientifiques de niveau recherche, publiés ou non, émanant des établissements d'enseignement et de recherche français ou étrangers, des laboratoires publics ou privés.

Copyright



Spectroscopy of B-type asteroids: Subgroups and meteorite analogs

Beth Ellen Clark,¹ Julie Ziffer,² David Nesvorny,³ Humberto Campins,⁴ Andrew S. Rivkin,⁵ Takahiro Hiroi,⁶ Maria Antonietta Barucci,⁷ Marcello Fulchignoni,⁷ Richard P. Binzel,⁸ Sonia Fornasier,⁷ Francesca DeMeo,⁷ Maureen E. Ockert-Bell,¹ Javier Licandro,^{9,10} and Thais Mothé-Diniz¹¹

Received 30 July 2009; revised 15 October 2009; accepted 16 December 2009; published 10 June 2010.

[1] B-type asteroids have a negative slope from ~ 0.5 to $\sim 1.1 \mu\text{m}$ and beyond. What causes this? Visible to near-infrared reflectance spectra ($0.4\text{--}2.5 \mu\text{m}$) are assembled for 22 B-type asteroids. The spectra fall naturally into three groups: (1) those with negative (blue) spectral shapes like 2 Pallas (7 objects), (2) those with concave curve shapes like 24 Themis (11 objects), and (3) everything else (4 objects). The asteroid spectra are compared to mineral and meteorite spectra from the Reflectance Experiment Laboratory library of 15,000 samples, in a least squares search for particulate analogs, constrained by spectral brightness. The Pallas group objects show a trend of analogs from the CV, CO, and CK meteorite groups. Only three of the seven Pallas-like objects are determined to be dynamically related (2, 1508, and 6411). The Themis group objects show a trend of analogs from the CI, CM, CR, CI-Unusual, and CM-Unusual meteorites (as expected from the work of Hiroi et al. (1996)). Seven of the 11 Themis-like objects are dynamically related (24, 62, 222, 316, 379, 383, and 431). Allowing for reasonable uncertainties in the spectral matches, we find no need to invoke mineralogies that do not exist in the meteorite collection to explain B-type spectra or their negative slopes. Our Themis group results are as expected and are consistent with previous work, but our Pallas group results are new and, in some cases, in conflict with previous work.

Citation: Clark, B. E., et al. (2010), Spectroscopy of B-type asteroids: Subgroups and meteorite analogs, *J. Geophys. Res.*, 115, E06005, doi:10.1029/2009JE003478.

1. Introduction

[2] In this study, we assemble, coordinate, and analyze visible and near-infrared wavelength spectral data of 22 B-type asteroids. By “B-type,” we mean any asteroid that has ever

been designated B or F in any of the commonly used taxonomies [Tholen, 1984; Bus and Binzel, 2002a, 2002b; Bus et al., 2008; DeMeo et al., 2009]. There are 116 such objects, so this collection of 22 represents 19% of known B types.

[3] Thirteen objects are newly observed and are presented in this work, while nine objects have been assembled from the previously published literature [Bell et al., 1988; Shepard et al., 2008; DeMeo et al., 2009]. Most targets were taxonomically designated based on visible wavelength spectral observations [Tholen, 1984; Bus and Binzel, 2002a, 2002b], and some were taxonomically designated based on near-infrared wavelength spectral observations [DeMeo et al., 2009]. B types are generally low-albedo asteroids (average around 7%), and their visible spectra have relatively flat, smooth characteristics, with weak/minor $1 \mu\text{m}$ absorptions attributed to iron-bearing silicates and gentle UV dropoffs [Tholen, 1984; Bus and Binzel, 2002b]. While B and F are distinct classes in the Tholen taxonomy [Tholen, 1984], more recent taxonomies merge the two into the B class because of differences in wavelength coverage. Tholen F types have UV absorption that differs from Tholen B types; however, the Bus taxonomy does not resolve these UV features [Bus and Binzel, 2002a, 2002b; DeMeo et al., 2009].

¹Department of Physics, Ithaca College, Ithaca, New York, USA.

²Department of Physics, University of Southern Maine, Portland, Maine, USA.

³Department of Space Studies, Southwest Research Institute, Boulder, Colorado, USA.

⁴Department of Physics, University of Central Florida, Orlando, Florida, USA.

⁵Applied Physics Laboratory, Johns Hopkins University, Laurel, Maryland, USA.

⁶Department of Geological Sciences, Brown University, Providence, Rhode Island, USA.

⁷Laboratoire d'Etudes Spatiales et d'Instrumentation en Astrophysique, Observatoire de Paris, Meudon, France.

⁸Department of Earth, Atmospheric and Planetary Sciences, Massachusetts Institute of Technology, Cambridge, Massachusetts, USA.

⁹Instituto de Astrofísica de Canarias, La Laguna, Tenerife, Spain.

¹⁰Departamento de Astrofísica, Universidad de La Laguna, La Laguna, Tenerife, Spain.

¹¹Observatório do Valongo, Universidade Federal do Rio de Janeiro, Rio de Janeiro, Brazil.

[4] A major goal of the present work is to see whether compositional analysis with recently obtained high-resolution visible-near-infrared spectra can improve on previously published findings (now about 14 years old) based on lower-resolution observations [e.g., *Hiroi et al.*, 1996]. Of curious importance is the nature and cause of the negative slope (from ~ 0.5 to $\sim 1.1 \mu\text{m}$) that characterizes B-type asteroids.

2. Background

[5] While the *Bus and Binzel* [2002b] visible wavelength taxonomy is consistent with that of *Tholen* [1984] for most of the major classes, there are differences in the details of minor asteroid classes. We note that *Tholen's* wavelength range (0.3–1.1) was longer than *Bus and Binzel's* (0.4–0.9), but the spectral resolution of *Bus and Binzel's* (187 channels) was higher than *Tholen's* (8 channels). In his taxonomy, *Tholen* [1984] described B, C, F, and G classes, using a combination of spectrum shape and albedo information. In their taxonomy, *Bus and Binzel* used only spectral shape (no albedo information), and they merged *Tholen's* B, C, F, and G classes, creating new classes B, Ch, Cg, Cb, and Cgh (see *Bus and Binzel* [2002b] or *Rivkin et al.* [2002] for a visual explanation of the class distinctions).

[6] Although B types exist in each of the currently used asteroid taxonomies (*Tholen*, *Bus*, and *Bus-DeMeo*), they are not as common as S types or C types among main belt or near-Earth asteroids. Their generally negative (blue) slopes are fairly unique and must be a strong constraint on their compositional properties. Only 4 B objects, of 371 objects (1%), are described in the recent paper presenting the *Bus-DeMeo* taxonomy [*DeMeo et al.*, 2009]. The *Tholen* taxonomy describes 7 B types (plus 11 B-ambiguous and about 50 F and F-ambiguous) of a total of 589 objects (12%), and the *Bus-Binzel* taxonomy describes 63 B types of 1190 objects (5%) [*Bus and Binzel*, 2002b]. There is considerable overlap among surveys; however, these numbers suggest that B types are more commonly found when only the visible wavelengths are observed.

[7] What is known about the composition of B-type asteroids? Tellingly, they do not show up as a source of meteorites on the summary chart by *Burbine et al.* [2002]. The blue slope of 2 Pallas was well known, but there is no obvious meteorite match in the published compendium of meteorite spectra by *Gaffey* [1976] (although the CV3 chondrite Grosnaja is the best candidate), and B types are missing from the summary chart by *Gaffey et al.* [2002]. Also, only one B type (2 Pallas) had been observed at $3 \mu\text{m}$ at the time of publication of the summary chart by *Rivkin et al.* [2002]. The fact that a hydration band was detected on Pallas was noted by these authors, with the footnote that Pallas may not be representative of the B class.

[8] Other low-albedo asteroid classes, such as the C types, have been generally linked with carbonaceous chondrite meteorites [*Burbine et al.*, 2002], and the B, C, G, and F asteroids have been proposed as comprising an alteration sequence [*Bell et al.*, 1989; *Vilas*, 1994]. *Rivkin et al.* [2002] reviewed the evidence in support of this idea, but conclusions are difficult because of small-number statistics. Note that fewer recent papers utilized *Tholen's* taxonomy exclusively and referred to the B, G, and F types as “subclasses”

of the C types [e.g., *Vilas et al.*, 1994; *Tholen and Barucci*, 1989].

[9] *Vilas and Gaffey* [1989], *Vilas* [1994], and *Vilas and Sykes* [1996] discussed the evidence that low-albedo asteroid surfaces have experienced heating with maximum temperatures high enough to mobilize water but not high enough to cause melting and recrystallization of the rocks. These studies were not specific to B types; however, they are highly relevant to low-albedo objects in general. *Vilas* [1994] showed that 6 of 18 *Tholen* B-type spectra tested positive for a spectral feature at $0.7 \mu\text{m}$. *Vilas and Gaffey* [1989] and *Vilas et al.* [1994] compared low-albedo asteroids to CI1 and CM2 carbonaceous chondrites, discussing analogs in the context of visible wavelength spectra.

[10] *Hiroi et al.* [1993, 1996] investigated the composition of the B, C, G, and F asteroids in more detail. These workers merged three wavelength regions of spectra of each of six asteroids in the *Tholen* B, C, G, and F classes that had been observed in the 8-color survey [*Zellner et al.*, 1985], the 52-color survey [*Bell et al.*, 1988], and the $3 \mu\text{m}$ region [*Jones et al.*, 1990; *Feierberg et al.*, 1985]. These extended spectra were then compared to meteorite spectra measured at the NASA Reflectance Experiment Laboratory (RELAB) facility at comparable wavelength coverage [*Hiroi et al.*, 1996]. *Hiroi et al.* [1996] found a good correlation between the spectral properties of the asteroids and CI, CM, CR, and CI/CM-Unusual chondrites. Using parameters that measured UV absorption, $0.7 \mu\text{m}$ absorption, and $3.0 \mu\text{m}$ absorption, these workers also found a good correlation between the asteroids and experimentally heated samples of the CM chondrite Murchison. The heated samples were grouped according to the state of phyllosilicates, where group 1 samples (heated to less than 400°C) were phyllosilicate rich, group 2 samples (heated to 400 – 600°C) showed phyllosilicates transforming to anhydrous silicates, and group 3 samples (heated to greater than 600°C) had become fully anhydrous. Similarities between the asteroids and the experimentally heated samples suggests that the B-, C-, G-, and F-type asteroids may have experienced various degrees of heating and/or thermal metamorphism of their surface materials. Although very convincing matches for C types and G types are shown in the paper by *Hiroi et al.* [1996], there is no direct comparison between 2 Pallas (the only B type used) and meteorite spectra.

[11] *Licandro et al.* [2007] presented 0.34 – $2.4 \mu\text{m}$ spectra of (Bus) B-type 3200 Phaethon and suggested compositional similarities with aqueously altered CI/CM meteorites and phyllosilicates such as montmorillonite and antigorite. Their results indicate that Phaethon is likely to be an “activated asteroid,” similar to the “main belt comets” [*Hsieh and Jewitt*, 2006].

[12] Recently, *Rivkin and Emery* [2008] presented 2.2 – $4.0 \mu\text{m}$ spectra of (Bus) B-type 24 Themis, showing evidence for water ice frost on an asteroid surface (this detection has been independently confirmed and found to be rotationally invariant by *Campins et al.* [2009]). Assuming a linear mix, *Rivkin and Emery* [2008] suggested that the implied surface area of the ice is up to 5%, a surprisingly large amount compared to comets. This detection presents a new problem in asteroid science: since water ice is not stable on the surface of 24 Themis over the age of the solar system, where does it come from? What does this imply about the interior

Table 1. Observational Circumstances

Object Number	Name	UT Date	Start (hh:mm)	T_{exp} (s)	Air Mass	Solar Analog
62	Erato	2008_07_15	09:01	300	1.10	Land 112–1333, Land 115–271
213	Lilaea	2008_03_11	10:42	100	1.01	Land 102–1081, Land 105–56
229	Adelinda	2008_09_25	06:28	720	1.31	Land 112–1333, Land 113–276, Land 115–271
261	Prymno ^a	2005_02_10	07:03	400	1.00	17 Hardorp (HD) stars
335	Roberta	2008_03_11	15:21	120	1.21	Land 102–1081, Land 105–56
379	Huenna	2008_07_15	09:50	240	1.36	Land 112–1333, Land 115–271
383	Janina	2008_09_25	07:16	720	1.30	Land 112–1333, Land 113–276 Land 115–271
419	Aurelia	2008_03_11	11:45	200	1.12	Land 102–1081, Land 105–56
426	Hippo	2008_03_12	09:08	340	1.15	64–Hyades, Land 97–249, Land 102–1081, Land 105–56,
505	Cava	2008_07_15	13:19	270	1.30	Land 112–1333, Land 115–271

^aThe spectrum of asteroid 261 Prymno was donated by Thais Mothé-Diniz and is included in the work of *Clark et al.* [2009].

of this asteroid? And why does 24 Themis not show cometary activity? We do not address these questions in the present work. We merely state them to indicate the ponderable nature of the Themis.

[13] Eponymous asteroid 24 Themis is also of great interest because of its membership in the Themis family. Themis family members are thought to be fragments of the largest known catastrophic collision in the asteroid belt. Several hundreds of Themis family members are known, and there may yet be more to be discovered. Of the known 116 B-type asteroids, 16 (i.e., 14%) are Themis family members [*Mothé-Diniz et al.*, 2005]. The parent body of the Themis family is calculated to have been ~450 km in diameter, comparable to Vesta [*Marzari et al.*, 1995]. The parent body was also probably water rich, so that Themis fragments such as 133P/(7968) Elst-Pizzaro show cometary activity when near their perihelion. *Nesvorný et al.* [2005] found visible-wavelength color trends between young and old asteroid families, using a disruption age for the Themis family of 2.5 Gy. *Ziffer et al.* [2008] have been targeting families with different disruption ages as a way of testing the relationship between the color of a primitive asteroid surface and its exposure age. So far, *Ziffer et al.* [2008] find that either (1) space weathering of primitive surfaces appears to make them “redder” in the near-infrared and less red in the visible or (2) the families examined so far began with distinctly different lithologies, and the relevance of color to space weathering is not so clear.

[14] Recovering a carbon-rich ureilite meteorite (ureilites are differentiated achondrite meteorites containing mostly olivine, pyroxene, and graphite, thought to come from S-type asteroids [*Gaffey et al.*, 1993]) after watching its approach to Earth as asteroid 2008 TC₃, *Jenniskens et al.* [2009] showed excellent agreement between the telescopic spectrum of the asteroid and subsequent laboratory spectroscopic measurement of the meteorite. This finding could indicate the following: (1) low-albedo featureless spectra are ambiguous (based on visible spectral properties alone, 2008 TC₃ might be interpreted to be a primitive chondritic object!), and (2) low-albedo materials may not be strongly altered by space-weathering processes [e.g., *Clark et al.*, 2002].

[15] Focusing on C-type asteroids, *Ostrowski et al.* [2009] reexamined the suggestion by *Hiroi et al.* [1996] of heated phyllosilicates as an analog material for low-albedo asteroids. In some recent experiments, *Ostrowski et al.* [2009]

have heated samples of common phyllosilicates, such as kaolinite, serpentinite, nontronite, montmorillonite, and chlorite, to various temperatures between 100°C and 1100°C. They describe the temperature at which phyllosilicates lose their chemically bound water (700°C). Measuring the resulting changes in the spectral continuum of these samples, *Ostrowski et al.* [2009] compared them with C types, confirming and extending the findings of *Hiroi et al.* [1996]. This work suggests that CM meteorites and many C-type asteroids have mineralogies similar to heated montmorillonite and kaolinite.

[16] In summary, the literature suggests that B-type asteroids may be composed of low-albedo, carbonaceous, and hydrated minerals (e.g., montmorillonite) such as are found in CM and/or CI chondrites. Some B types may have also experienced some heating and/or thermal metamorphism, as has happened to the Unusual CI and CM meteorites [*Hiroi et al.*, 1993, 1996]. Previous results suggest that spectroscopically mixing mineral end-members to simulate carbonaceous chondrites and/or low-albedo asteroids may be complicated by the additional free parameter of the thermal history of end-member minerals. The 2008 TC₃ ureilite also indicates that some low-albedo materials may not require space-weathering alteration to match their asteroid parent body spectra, particularly for non-main-belt objects. It follows that compositional studies of low-albedo asteroids, for the time being, are perhaps best constrained by meteorites existing in our Earthly collections.

3. Observations

[17] New observations were conducted at the Mauna Kea Observatory 3.0 m NASA Infrared Telescope Facility in Hawaii (see Table 1). We used the SpeX instrument, equipped with a cooled grating and an InSb array (1024 × 1024) spectrograph at wavelengths from 0.82 to 2.49 μm [*Rayner et al.*, 2003]. Spectra were recorded with a slit oriented in the north-south direction and opened to 0.8 × 15 arcseconds. A dichroic lens reducing the signal below 0.8 μm was used for all observations. Objects were consistently observed near the meridian to minimize air mass, but total integration time varied from 20 min to 2 h, depending on the strength of the signal relative to sky lines.

[18] Following normal data reduction procedures of flat-fielding, sky subtraction, spectrum extraction, and wavelength calibration, each spectrum was fitted with an

Table 2. Asteroids Considered in This Study^a

Name	Tholen Class	Bus Class	Bus-DeMeo Class	p_v	IR Data Source	a (AU)	Family	Diameter (km)	VIS	NIR1	NIR2	BC	BD	
2	Pallas	B	B	B	0.16	Bus	2.77	2	532	-0.01	-0.17	-0.05	1.28	0.05
24	Themis	C	B	C	0.07	Ziffer	3.13	24	198	-0.10	0.02	0.17	1.26	0.08
62	Erato	BU	Ch	B	0.06	Clark	3.12	24	95.4	-0.22	0.01	0.08	1.21	0.08
213	Lilaea	F	B	B	0.09	Clark	2.75		83.0	-0.09	-0.11	-0.04	1.50	0.03
222	Lucia	BU	-	-	-	Ziffer		24	-	-	-0.05	0.08	-	-
229	Adelinda	BCU		X	0.05	Clark	3.42		93.2	0.01	0.32	0.36	0.86	0.05
261	Prymno	B	X	X	0.11	Clark	2.33		50.9	0.28	0.30	0.13	0.91	0.02
316	Goberta				-	Ziffer		24	-	-0.04	-0.04	0.05	1.55	0.03
335	Roberta	FP	B	C	0.06	Clark	2.47		89.1	-0.04	0.04	0.09	1.17	0.05
379	Huenna	B	C	-	0.06	Clark	3.13	24	92.3	-0.09	0.18	0.22	1.09	0.06
383	Janina	B	B	C	0.09	Clark	3.15	24	45.5	-0.24	0.05	0.04	1.08	0.07
419	Aurelia	F	-	C	0.05	Clark	2.59		129	0.06	0.01	0.13	1.26	0.04
426	Hippo	F	-	B	0.05	Clark	2.89		127.1	0.05	-0.25	-0.03	1.73	0.08
431	Nephele	B	B	C	0.06	Ziffer	3.14	24	95.0	-0.11	0.09	0.22	1.18	0.09
505	Cava	FC	-	Xk	0.04	Clark	2.69		115	0.38	0.20	0.19	0.95	0.07
554	Peraga	FC	Ch	Ch	0.05	Bell	2.37		95.9	0.12	0.09	-0.02	1.16	0.03
704	Interamnia	F	B	C	0.07	Bell	3.06		316.6	-0.15	-0.04	0.18	1.35	0.13
762	Pulcova	F			0.05	Bell	3.15		137.1	0.01	-0.07	0.13	1.59	0.05
1508	Kemi	BCF	C	B	-	Binzel	2.77	2	-	0.04	-0.06	-0.01	1.22	0.04
2100	RaShalom 1	C	Xc	B	0.0600.06	Shepard	0.08		3.4	0.35	0.02	-0.03	1.04	0.03
2100	RaShalom 2	C	Xc	B	0.06	Shepard	0.08		3.4	0.18	-0.04	-0.07	0.97	0.03
3200	Phaethon	F	B	B	0.11	Binzel	0.89		1.27	-0.42	-0.19	-0.04	1.29	0.15
6411	Tamaga	-	-	BBBB	-	Binzel	2.76	2	-	-0.04	-0.14	-0.10	-	-

^aThe infrared (IR) spectra of asteroids 2, 1508, 3200, and 6411 were published by *DeMeo et al.* [2009]. The infrared spectra of asteroids 261, 379, 213, 335, 419, 426, and 505 were published by *Clark et al.* [2009]. Visible (VIS) and infrared spectra of the two longitudes of 2100 were published by *Shepard et al.* [2008]. Visible wavelength spectra of 316 and 762 were obtained from S3OS2 [Lazzaro et al., 2004]. Visible wavelength spectra of 419 are from *Lazzarin et al.* [2001]; all other visible spectra are from the Small Main Belt Asteroid Spectroscopic Survey [Bus and Binzel, 2002a], the 24-color survey [Chapman and Gaffey, 1979], or the 8-color survey [Zellner et al., 1985]. Diameters, heliocentric distances (a), and geometric albedos (p_v) are from the JPL Horizons online database (ssd.jpl.nasa.gov). Family membership is according to the dynamical research conducted for this study (D. Nesvorný). See text for descriptions of BC, BD, VIS, NIR1, and NIR2. Errors in band measurements are not reported here, for simplicity, but are available upon request. See the study of *Ockert-Bell et al.* [2008] for a discussion of errors. AU, arbitrary units.

atmospheric transmission (ATRAN) model for telluric absorption features [Lord, 1992; Bus et al., 2003; Sunshine et al., 2004]. This procedure required an initial estimate of precipitable water in the atmospheric optical path using the zenith angle for the observation and the known τ values (average atmospheric water) for Mauna Kea. This initial guess was iterated until the best fit between predicted and observed telluric band shapes was obtained and an atmospheric model spectrum was generated [Bus et al., 2003]. Following this, each asteroid spectrum was divided by the atmospheric model and ratioed to each star spectrum, similarly reduced, before normalization at 1.2 μm . The software and procedures used for data reduction are neatly described by *DeMeo et al.* [2009].

[19] The final spectra we report are averages of three to five asteroid/star ratios, calculated to minimize variations caused by standard star and sky variability. Usually, two to five different standard stars were observed on any given night at the telescope (Table 1). We used only “solar” standard stars, and each standard star was observed one to three times per night across different air masses.

[20] To maximize our compositional analysis, we assembled additional B-type asteroids from the literature. Table 2 gives a summary of the assembled asteroid data. Several objects are worth special mention. The 2100 Ra Shalom asteroid was heavily observed across multiple wavelengths and was determined to be most closely linked with CV meteorites by *Shepard et al.* [2008]. We include it here because the Bus-DeMeo online taxonomy calculator assigns a B-type designation. Although 3200 Phaethon has been

observed by *Licandro et al.* [2007], the spectrum reported here comes from *DeMeo et al.* [2009].

4. Results

[21] Figures 1–3 present our target spectra. Where possible, visible wavelength data from the Small Main Belt Asteroid Spectroscopic Survey, Eight Color Asteroid Survey (ECAS), 24-color asteroid survey, or S³OS² survey are spliced to the near-infrared spectra and displayed normalized to 1.0 at 0.55 μm [Bus and Binzel, 2002b; Zellner et al., 1985; Chapman and Gaffey, 1979, Lazzaro et al., 2004, respectively]. To splice the data, we used the flux-normalized visible wavelength spectrum as the basis and applied a multiplicative scale factor to the infrared data until we found the best fit in the overlap wavelengths. If there is no continuity in the overlap region (e.g., asteroid 379 Huenna), then we use the center of the overlapping wavelengths as the tack point. We do not smooth, bin, or truncate any data.

[22] We measured and recorded relative brightnesses, absorption band depths and centers, and continuum slopes of the combined spectra (Table 2). The meteorite absolute reflectance at 0.55 μm is assumed to be roughly comparable to asteroidal geometric albedo. Although the numbers are obtained through different methods, they both measure relative brightness and have the same possible range of 0–1.0. We consider both measurements to be indicative of the overall spectral “brightness” of the compositional material. *Clark et al.* [2001, 2002] and *Fanale et al.* [1992] discussed the strength and viability of this assumption, especially in

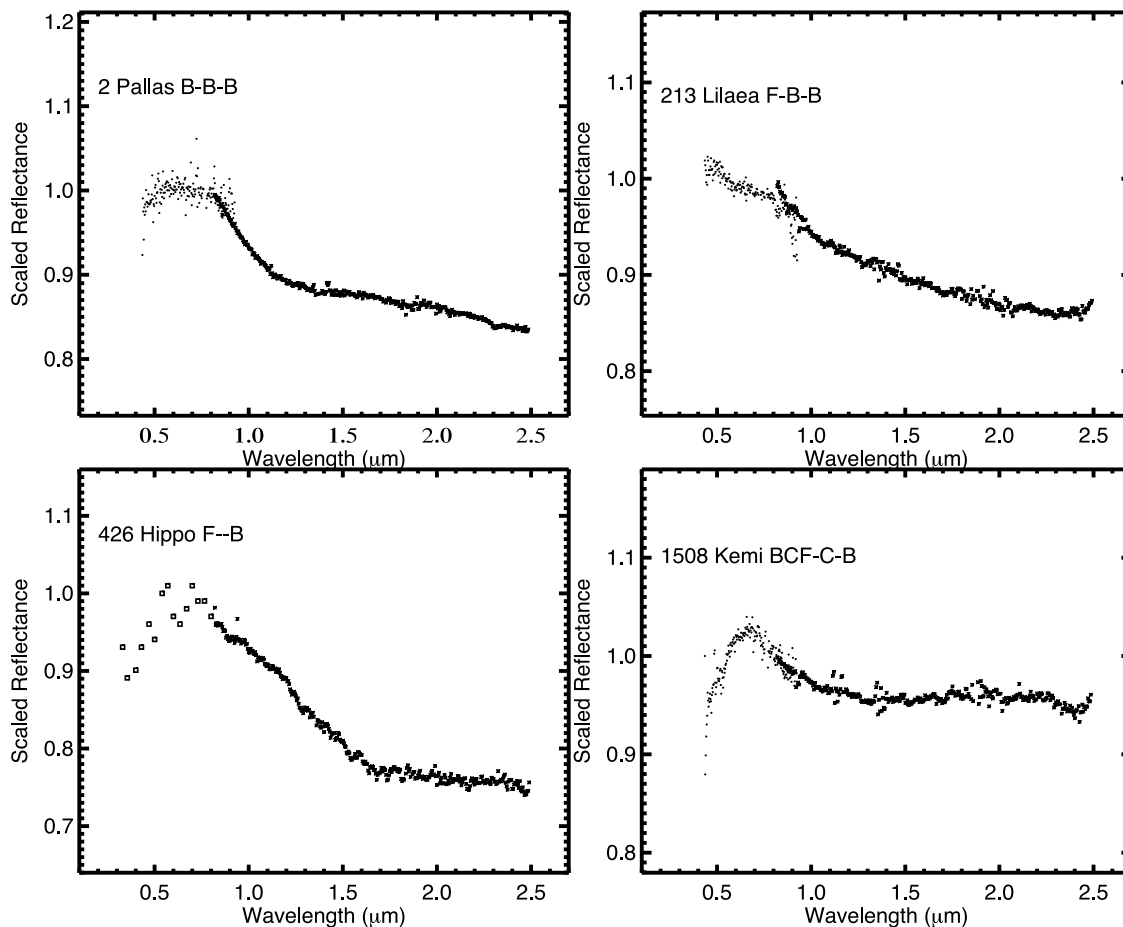


Figure 1. Pallas group. Each asteroid is shown relative to its own normalized reflectance at $0.55 \mu\text{m}$. Next to the name are the taxonomic designations of the asteroid in three different systems as follows: Tholen-Bus-BusDeMeo. Note that Pallas is the only asteroid that retained the B class designation through all taxonomic systems (for most systems, it defined the B type). Visible wavelength data are from the Small Main Belt Asteroid Spectroscopic Survey 2 [Bus and Binzel, 2002a] (small circles), 24-color survey [Chapman and Gaffey, 1979] (small squares), and 8-color survey [Zellner et al., 1985] (very small squares). Visible wavelength data of asteroid 316 are from S^3OS^2 [Lazzaro et al., 2004], and visible data of asteroids 419 and 762 are from *M. Lazzarin et al.* [2001]. Infrared wavelength data (crossed stars) are assembled for this paper, and their sources are listed in Table 2.

the context of disk-resolved observations of an asteroid regolith.

[23] Band center positions were measured after continuum removal to the center of a third-, fourth-, or fifth-order polynomial fit to the band. Band depths are measured as percentage depths from the continuum to the band center (unitless). Our technique for estimating the uncertainties in our band parameters was outlined by *Ockert-Bell et al.* [2008] and *Clark et al.* [2009]. We measure only the broad absorption band centered near $\sim 1.1\text{--}1.3 \mu\text{m}$. Also visible in our spectra are two other basic features: (1) a UV absorption below $\sim 0.5 \mu\text{m}$, and (2) a $0.7 \mu\text{m}$ absorption. The absorption below $0.5 \mu\text{m}$ is attributed to a ferric oxide intervalence charge transfer transition and is composed of multiple absorptions in the blue/UV spectral region. This feature is common to all iron-silicate materials. We do not resolve the shorter wavelength end of this band. The absorption band at $0.7 \mu\text{m}$ has been attributed to oxidized

iron (Fe^{2+} to $>\text{Fe}^{3+}$) in phyllosilicate minerals [Vilas and Gaffey, 1989; Hiroi et al., 1996]. This band occurs in laboratory spectra of phyllosilicate-bearing materials, is independent of the particle size of a sample, and has been detected at the level of about 5% in asteroid spectra.

[24] We made several measurements to quantify the variation in the data. The continuum slope was measured as rise over run of the least squares linear fit to the data (change in normalized reflectance divided by change in wavelength; units are in μm^{-1}). The continuum slope was measured for four wavelength regions; visible was from 0.5 to $0.8 \mu\text{m}$, near-infrared (NIR1) was from 0.9 to $1.4 \mu\text{m}$, and near-infrared (NIR2) was from 1.5 to $2.4 \mu\text{m}$. The slopes in these three spectral regions capture the shape of the spectra reasonably well.

[25] We find that we can divide the spectra into three broad groups based on the behavior of the long-wavelength end of the near-infrared spectra, or NIR2.

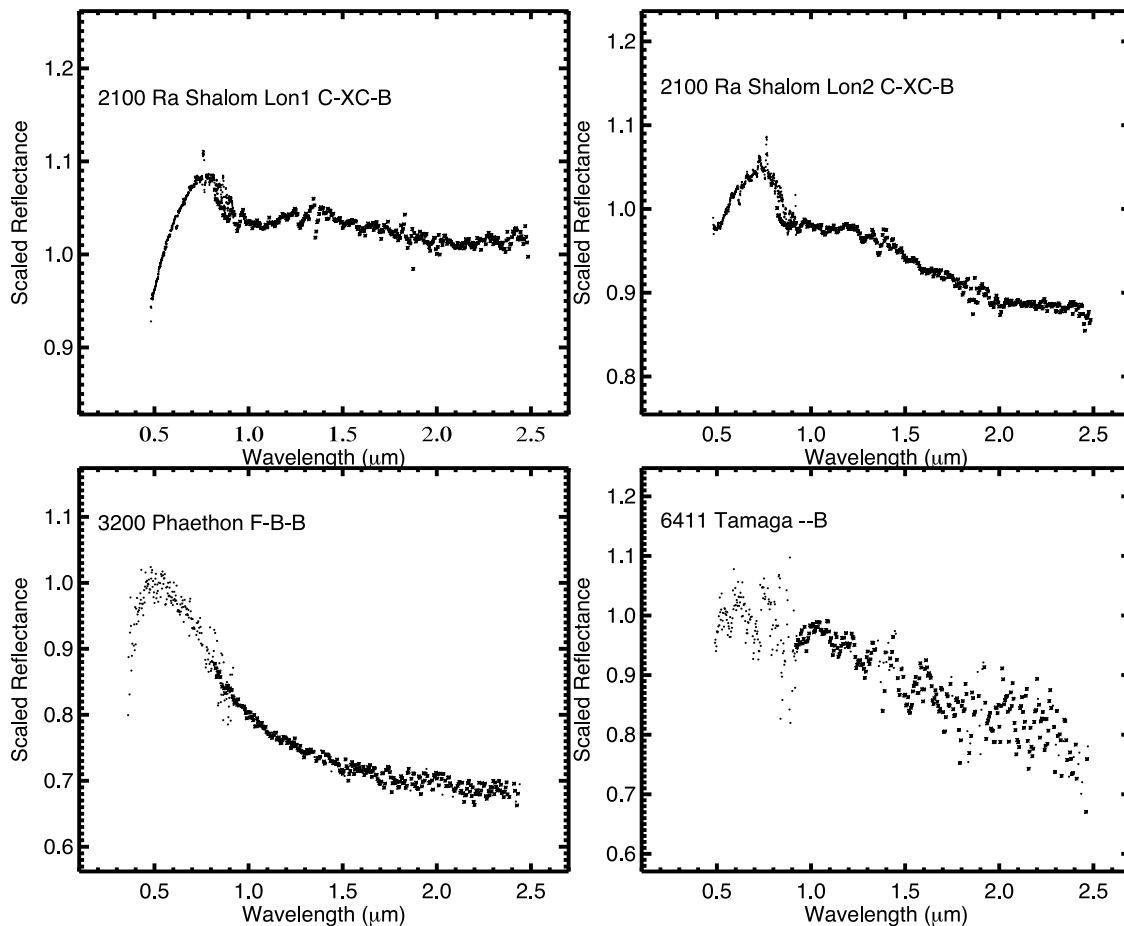


Figure 1. (continued)

[26] Figure 1 presents all asteroids with negative slopes from the peak in the visible wavelengths ($\sim 0.6\text{--}0.7\ \mu\text{m}$) to the long-wavelength end of the survey ($\sim 2.5\ \mu\text{m}$). These objects are all identified as B types according to the Bus-DeMeo decision tree from *DeMeo et al.* [2009] via the online taxonomic calculator (<http://smass.mit.edu/busdemeoclass.html>). We call this the Pallas group.

[27] Figure 2 presents asteroids with what appear to be very broad absorption bands centered variously from 1.1 to $\sim 1.3\ \mu\text{m}$. These objects were mostly identified as C types in the online Bus-DeMeo taxonomic classification utility. We call this the Themis group. Broad absorption bands near $1.1\text{--}1.3\ \mu\text{m}$ have been found in other asteroids, notably 1 Ceres, 52 Europa, and 85 Io [see *DeMeo et al.*, 2009].

[28] Figure 3 presents all asteroids that did not fall into the first or second groups above. We call this the Other group.

4.1. Analog Search

[29] To constrain the possible mineralogies of our asteroids, we conducted a search for meteorite and/or mineral spectral matches. We used the publicly available RELAB spectrum library [*Pieters*, 1983], which consisted of nearly 15,000 spectra in November 2008. For each spectrum in the library, a filter was applied to find relevant wavelengths

($0.4\text{--}2.5\ \mu\text{m}$). Then, a second filter was applied to reject spectra with irrelevant albedo values (brightness at $0.55\ \mu\text{m}$). This process produced a list of approximately 4000 RELAB spectra of appropriate brightness and wavelength coverage for comparison to the asteroid. RELAB spectra were normalized to 1.0 at $0.55\ \mu\text{m}$, and a χ^2 value was calculated relative to the normalized input asteroid spectrum. The list was sorted according to χ^2 and visually examined for dynamic weighting of spectral features by the spectroscopist. Given similar χ^2 values, a match that mimicked spectral features was preferred over a match that did not. We visually examined the top ~ 200 χ^2 matches for each asteroid (or until the χ^2 increased beyond an acceptable range, usually around 30% of the lowest value). After selection of the top analogs based on quality of fit, a third filter was applied to reject nonparticulate samples. No specific grain-size sampling was applied, but most meteorite matches found by this method tended to have grain sizes less than $125\ \mu\text{m}$.

[30] We tested a variety of methods to deal with the fact that a material's albedo dominates its spectral properties. We tried a grid search over the χ^2 results in albedo increments of 0.01 (too much human intervention); we tried fixing the albedo at the upper, middle, and lower ends of an absolute range of 10% (missed too many spectral matches); and we

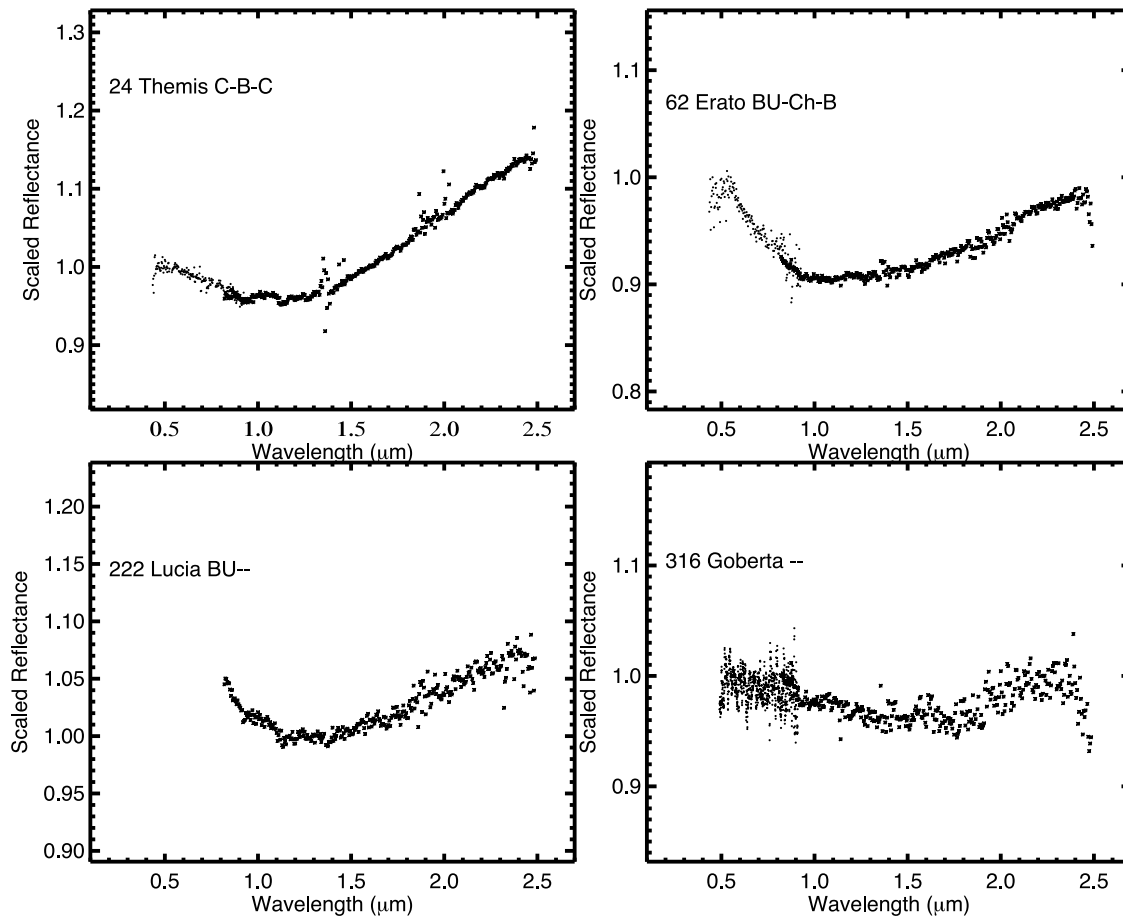


Figure 2. Themis group. For plotting details, see caption of Figure 1.

tried normalizing everything and ignoring albedo unless it was wildly different (albedo is a strong constraint and should be used). Finally, we decided to constrain the search for analogs to those laboratory spectra with brightness (reflectance at $0.55 \mu\text{m}$) roughly comparable to the albedo of the asteroid. For the asteroid albedo value, we generally used the IRAS albedo published by *Tedesco et al.* [2002]. For the darker asteroids (below 10% albedo), this is a fairly well-known number. The uncertainty for brighter asteroid albedos (above 10% albedo) is relatively larger. This is because at equivalent geocentric and heliocentric distances, a darker asteroid will have stronger thermal flux, allowing a more precise and more accurate albedo determination. To account for this, we filtered out laboratory spectra if brightness differed by more than $\pm 3\%$ in absolute albedo for the darker asteroids (albedos less than 10%), and we filtered out laboratory spectra if brightness differed by more than $\pm 5\%$ in absolute albedo for the brighter asteroids (albedos greater than 10%). For example, if an asteroid's albedo was 10%, we searched over all laboratory spectra with $0.55 \mu\text{m}$ reflectance between 5% and 15%. Once the brightness filter was applied, all materials were normalized before comparison by least squares.

[31] Our search techniques effectively emphasized the spectral characteristics of brightness and shape and de-emphasized minor absorption bands and other parametric

characteristics. As such, we suggest that our methods are complimentary to the band parameter studies performed by others.

[32] Results of the search are presented as a matrix in Table 3, and some of the fits are graphed in Figures 4 and 5. The matches we present were the “best” fits we could find from the RELAB database; however, in the absence of ground truth, we cannot make claims about their accuracy. In general, we found reasonable spectral analogs for most asteroids in our sample. The Pallas group objects had higher χ^2 fit values and tended to be best fit with CK, CV, or CO materials. Asteroid 2 Pallas was best fit with CK meteorites, probably because these meteorites have brighter albedos and more negative slopes from 0.7 to $2.5 \mu\text{m}$ than other carbonaceous chondrites. However, there are some problems with the Pallas-CK match. We note that the CK meteorites have an absorption band at $\sim 1 \mu\text{m}$ that is basically absent in Pallas and that a $3 \mu\text{m}$ band indicating hydrated minerals (phyllosilicates) has been detected on Pallas [*Rivkin et al.*, 2002], in conflict with the phyllosilicate-free CK meteorites. In the summary table of meteorite parent bodies in the work of *Burbine et al.* [2002], we find that CK meteorites are linked to C asteroids described by *Gaffey and McCord* [1978]; however, more recent work by *Mothe-Diniz et al.* [2008] shows evidence for a link with K-type asteroids of the Eos family. In our first RELAB search, asteroid 2 Pallas

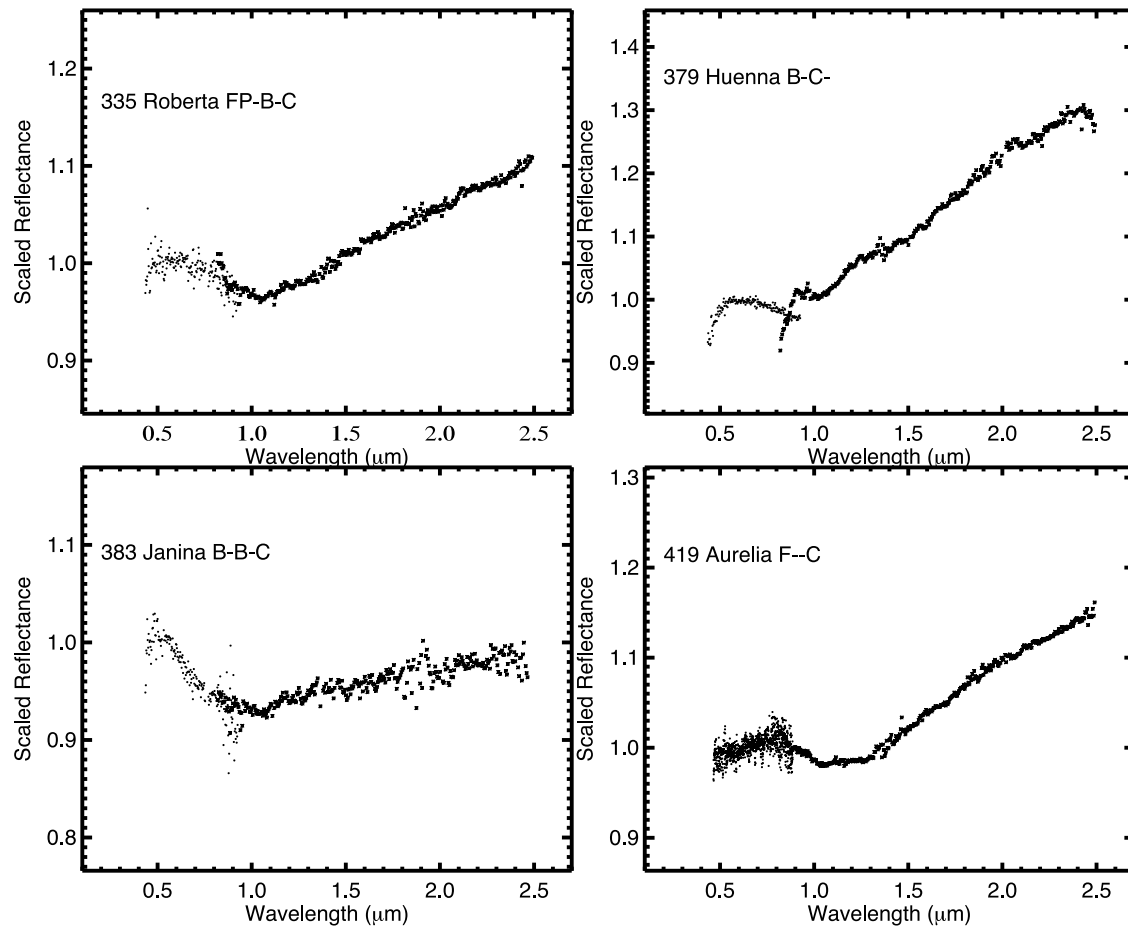


Figure 2. (continued)

was actually exceptionally well fit by a basalt slab specimen, but we decided that such an analog was unlikely, partly based on the polarization data that strongly indicate particulate surfaces for most large main belt asteroids like Pallas [e.g., Belskaya *et al.*, 2009; Fornasier *et al.*, 2006], and based on the thermal inertia data that also indicate particulate surfaces [Delbó *et al.*, 2007]. Asteroid 1508 Kemi was best fit with a diogenite specimen (diogenites are differentiated achondrite meteorites containing mostly orthopyroxene, which is thought to come from asteroid 4 Vesta [Consolmagno and Drake, 1977]), a coarse grain-size sample of Kaidun, and an experimentally produced sample of heated olivine. According to the Meteoritical Society (<http://tin.er.usgs.gov/meteor/metbull.php>), Kaidun is a CR chondrite. Apparently, however, there is some controversy over this classification. Some workers claim that Kaidun has a wide range of primitive CM-like materials and may be a breccia [e.g., Zolensky *et al.*, 1996]. Thus, Kemi seems to be spectrally consistent with a fairly wide range of mineralogies. Asteroid 3200 Phaethon was best fit with CK meteorites or an experimental mixture of chlorite and carbon lampblack. The CK interpretation conflicts with the suggestions of Licandro *et al.* [2007] for 3200 Phaethon, namely, Unusual CM chondrites, experimentally heated CI chondrites, or mixtures of montmorillonite or antigorite with carbon lampblack. Our chlorite and lampblack fit is more

consistent with Licandro *et al.* [2007], and chlorite is a phyllosilicate commonly found in meteorites. Our spectrum of asteroid 6411 Tamaga was very noisy and therefore allowed many different kinds of fits.

[33] The Themis group objects tend to be best fit with CM, CI, CR, CM/CI Unusual meteorites, and/or heated CM/CI samples. Of the top 30 matches presented, 19 are of heated or Unusual (thermally metamorphosed) material. This seems to support the conclusion by Hiroi *et al.* [1993, 1996] that thermally metamorphosed materials are good analogs for some of the low-albedo (C-, G-, B-, and F Tholen-type) asteroids. We note that 50% of our Themis group are consistent with thermally metamorphosed material. It is interesting, then, that the fraction of CI, CM, and CR chondrites in the collection that are thermally metamorphosed is about 64 weight% [Yanai and Kojima, 1995]. A heated olivine sample matched asteroids 24 Themis, 316 Goberta, and 704 Interamnia. Indeed, the heated olivine sample seems to be the best sample for faithfully mimicking band features as well as the long wavelength redness of our asteroids. Notice the problem that all meteorite matches have in mimicking the long-wavelength redness of asteroid 431 Nephela. According to RELAB, the heating of the olivine sample is not specifically defined in terms of temperature or atmospheric conditions. This presents a problem for comparison to asteroids; however, given the unexpected detection of

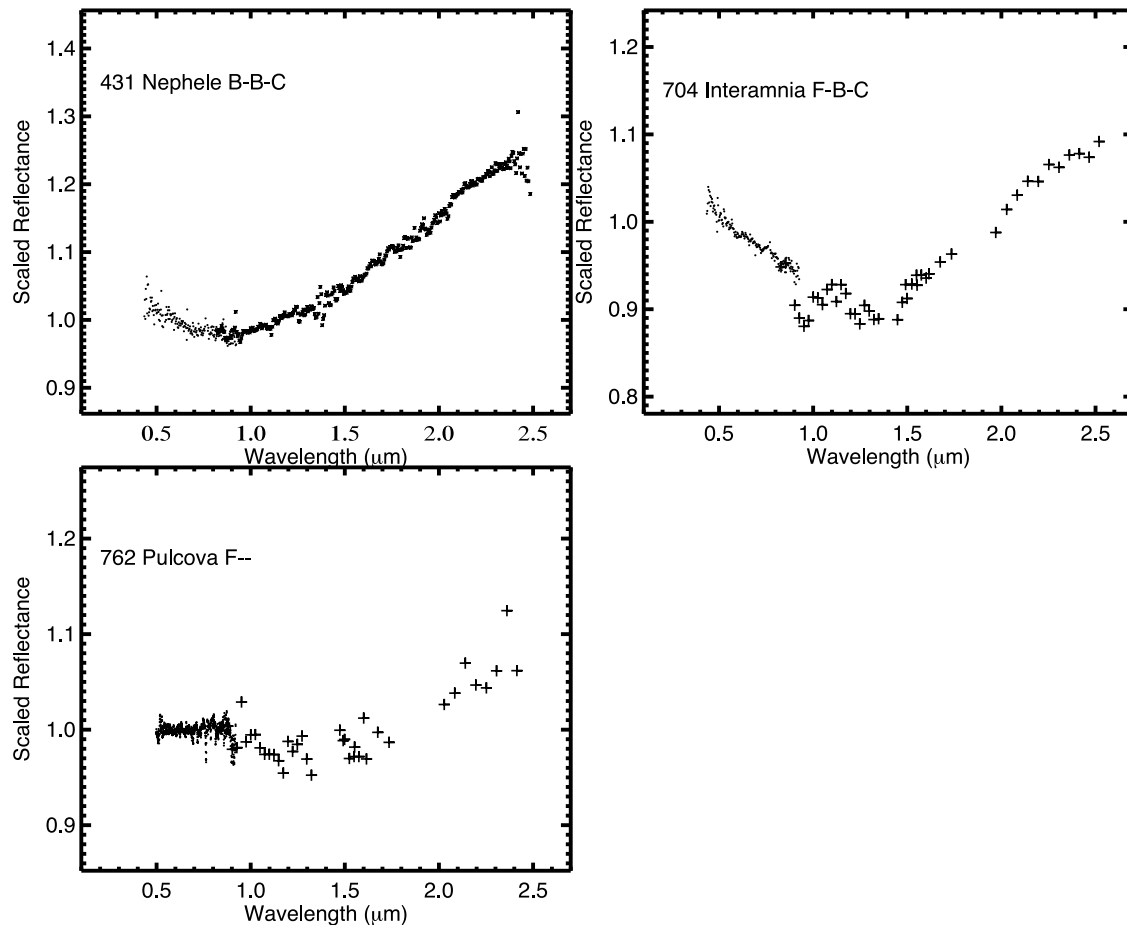


Figure 2. (continued)

water ice frost on asteroid 24 Themis [Rivkin and Emery, 2008; Campins *et al.*, 2009], we decided not to rule out the possibility that heated olivine is an analog material for these asteroids. We believe that more investigation is required before we can be certain of this identification. Note that Themis group member 222 Lucia was not fit with laboratory spectra because we did not have the critical visible wavelength portion of the spectrum.

[34] Among the Other asteroids, we note that asteroid 554 Peraga (Bus-DeMeo Ch type), which has a distinct $0.7 \mu\text{m}$ phyllosilicate absorption feature, was best fit with the CI chondrite Y-86029, measured at a grain size $<125 \mu\text{m}$ (Table 3). Although the near-infrared spectral data for this object are noisy, this result is consistent with many previous investigations that have identified phyllosilicate-rich meteorites as analogs for asteroids showing this $0.7 \mu\text{m}$ feature [e.g., Fornasier *et al.*, 1999; Vilas and Gaffey, 1989; Vilas *et al.*, 1993, 1994].

[35] In summary, we find that if we allow for uncertainties attributed to (1) grain sizes of asteroid surfaces and (2) disparate measurements of albedo and reflectance, we can find satisfactory spectral matches for most of the asteroids in our sample without invoking unsampled meteorite lithologies. We emphasize that the ensemble matches (those found between groups of asteroids and groups of meteorites) are probably a stronger argument for relatedness than any indi-

vidual match. This is consistent with the recent trend in asteroid-meteorite studies of allowing for “mixtures” of meteorite and/or mineral spectra to model an asteroid spectrum [e.g., Mothé-Diniz *et al.*, 2008].

4.2. Dynamics

[36] Given the three groups we have found in the B-type sample so far, it is reasonable to ask the question: Could the members of each group be dynamically related to one another? Because of the rate of asteroid discoveries, every year or so the asteroid ephemerides catalog is reanalyzed for family relationships. Orbital elements of asteroids in our sample are compared to other asteroids and with known families. The process is automated to allow for rapid updates, and new families are frequently discovered. The catalog we used has 181,210 numbered asteroids in total. Results for the Themis family were published previously [Nesvorný *et al.*, 2008; J. Ziffer *et al.*, manuscript in preparation, 2010], and results for Pallas are discussed here.

[37] In the Pallas group, 2100 Ra Shalom and 3200 Phaethon are both highly evolved near-Earth asteroids, so it is not clear where they have come from. The 426 Hippo asteroid seems to have a normal main belt orbit, except for a relatively high inclination.

[38] Pallas has a family with 69 members. Table 4 presents a list of synthetic proper elements for the dynamical

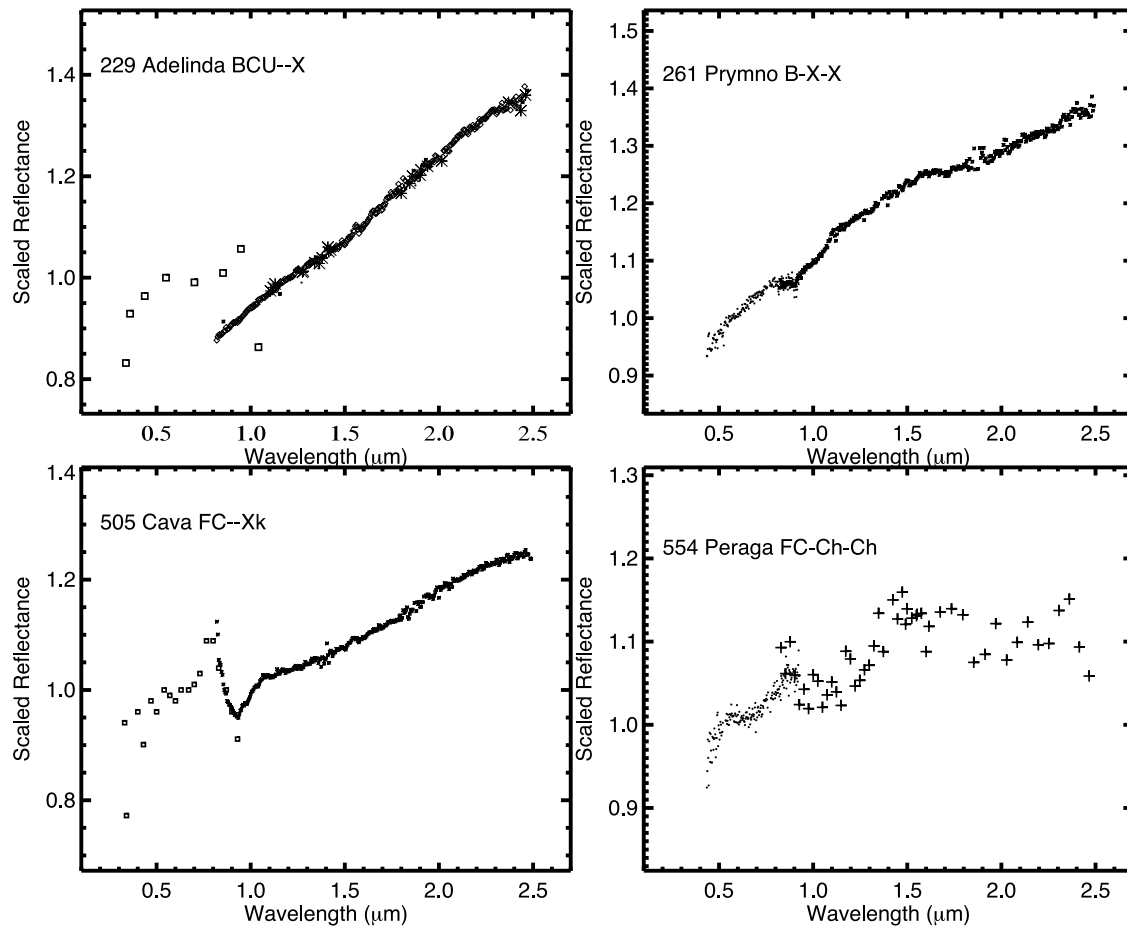


Figure 3. Other group. For plotting details, see caption of Figure 1.

core of the family. With a looser cutoff, the list would probably be larger. Of the first eight asteroids on the family list, seven have been observed in the *Bus and Binzel* [2002b] survey, and all seven objects were classified as Bus B types (somebody needs to look at 4969 and at everything beyond 5330). This would indicate some degree of compositional homogeneity in the family. It would be instructive to take a look at the Sloan Digital Sky Survey colors for Pallas family objects to see whether this trend persists when more family members are included.

[39] The disruption age of Pallas is difficult to determine mainly because of unknown (and possibly large) ejection speeds that become confused with Yarkovsky spreading. We have used a generous cutoff to include as many members as possible. Most members in Table 4 have been discovered since 2002. From a dynamical standpoint, the Pallas family is one of ~ 5 – 10 high-orbital-inclination families ($i > 17^\circ$). The family is very well defined dynamically mainly because there are very few background asteroids with high-orbital inclinations. This has been interpreted to indicate that there were only a few asteroids with high i originally and that most of them have been collisionally disrupted over the past 4 Gy. In contrast, in the low main belt ($i < 17^\circ$), the background asteroid population seems to represent a large fraction of the total population ($\sim 50\%$). It is interesting to

speculate on what this is telling us about main belt formation and evolution.

[40] Figure 6 shows the orbital distribution of asteroids with the Pallas family in red. Note that in the (a,e) plot, only orbits with $i > 20^\circ$ are plotted (to get rid of the many objects with $i < 20^\circ$). Figure 7 shows the cumulative size-frequency distribution (SFD) of the Pallas family (black) and a sample smooth particle hydrodynamics (SPH) run (dashed line). We assumed albedo $A = 0.15$ and a diameter of 2 Pallas $D = 550$ km. The SFD indicated is fairly characteristic for cratering impact on a large parent body: starting at $H = 11$, the distribution steeply rises with smaller objects. The total volume of fragments corresponds to an object ~ 33.4 km in diameter. SPH simulations of cratering impacts look the same [Durda *et al.*, 2007]. There are some puzzling aspects of the size-frequency distribution of the Pallas family. For example, there is a large gap between Pallas and the second largest asteroid in the family. This could indicate a cratering event; however, the size distribution below the size of the second fragment ($D < 20$ km) is rather shallow compared to SPH simulations. In Figure 7, the solid line denotes the family SFD, and the dashed line is a best SPH fit to the first and second fragments. One can see that the SPH distribution is significantly steeper for $D < 20$ km. Possible explanations include the following. (1) SPH simulations were done on $D = 100$ km targets from solid basalt. Pallas is much larger, so

Table 3. RELAB Search Results: Top Three for Each Asteroid^a

Number	Name	Summary	1			2			3					
			Best Fit	Ref (0.55)	Grain Size (μm)	RELAB File	Best Fit	Ref (0.55)	Grain Size (μm)	RELAB File	Best Fit	Ref (0.55)	Grain Size (μm)	RELAB File
<i>Group 1, Pallas, B Type</i>														
2	Pallas	CK	CK5/6	0.13	part	c1lm19	CK5	0.13	<125	lmmb92	CK5	0.15	<63	c1mp03
213	Lilaea	CV	CV3	0.06	75–150	egp130	Heated Oliv	0.07	part	clao01	CV3	0.11	<125	lamt16
426	Hippo	CV	CV3	0.06	150–500	mgp132	CM Unusual	0.09	<125	c1mp55	CV3	0.06	75–150	egp130
1508	Kemi	CR	HED	0.04	<25	bkr1mp113	CR Kaidun	0.04	>250	c2ma76	Heated Oliv	0.06	<250	c2ao02
2100	RaShalom	CV	CV3	0.11	<75	egp128	CV3	0.08	<300	egp138	CO3	0.09	<300	egp102
2100	RaShalom	CO	CO3	0.06	150–500	egp106	CV3	0.07	63–125	c4mb63	CO3	0.09	<300	egp102
3200	Phaethon	CK	CK4	0.09	75–125	cdmb81	CK4	0.11	<250	name03	Chlorite+Carb	0.09	<125	c1xt55
6411	Tamaga	?	CI	0.04	<125	c4mb60	CM2	0.04	<125	c4mb61	CV3	0.06	150–500	egp132
<i>Group 2, Themis, C Type</i>														
24	Themis	CM Unusual	Heated Oliv	0.07	<250	c5ao02	CM Unusual	0.06	<125	ncmp10	Heated CM	0.06	<63	ncmb64f
62	Erato	CM	CM	0.06	<125	c1mb20	CR Kaidun	0.04	>250	bkr2ma076	CM Anom	0.04	part	c1ma78
316	Gobera	CM	Heated Oliv	0.06	<250	c4ao02	CM	0.04	part	c1ma78	CM Unusual	0.06	<125	ncmb20
335	Roberta	CM/CI Unus	Heated CM	0.06	<63	ncmb64f	CM Unusual	0.06	<125	ncmp10	CI Unusual	0.04	<125	c1mb19
379	Huenna	CM	Oxide Wust	0.04	<63	c1sc13	CM2	0.05	<125	bkr1mp02210	CM2	0.05	<125	c1mp11
383	Janina	CM	CM Unusual	0.06	<125	ncmb20	CM1	0.05	<75	c1ph43	Heated CM	0.07	<63	ncmb64g
419	Aurelia	CM Heated	Heated CM	0.06	<63	ncmb64f	Heated CI	0.03	<125	egmp18	CM2	0.03	<500	c1me02
431	Nephele	CM	CM2	0.03	<500	name02	Heated CM	0.06	<63	cfmb64	CM2	0.05	<125	ncmp11
704	Interammia	CI Unus	CI Unusual	0.04	<125	ncmb19	Heated CM	0.05	63–125	cmmb64	Heated Oliv	0.07	<250	c5ao02
762	Pulcova	CM Unus	CM Unusual	0.06	<125	ncmp10	Heated CM	0.06	<63	cfmb64	CM	0.09	part	bkr1ma077
<i>Group 3, Other, X Type</i>														
229	Adelinda	CM	CM2	0.05	<75	egp092	Heated CM	0.03	<63	ncmb64c	CM2	0.05	<75	c1ph51
261	Prymno	OC	OC LL5	0.06	<300	cgm151	CR2	0.07	<100	c1mb58	E4	0.07	<125	c1mb40
505	Cava	OC	OC L6	0.08	<63	s2mp01	CM Unusual	0.05	<125	c2mb18	Ureilite	0.07	45–75	ccmb87
554	Peraga	?	CI	0.03	<125	c3mp111	E4	0.08	<125	cgmt40	OC L6	0.08	<63	s1mp01

^aPresented by Asteroid Group.

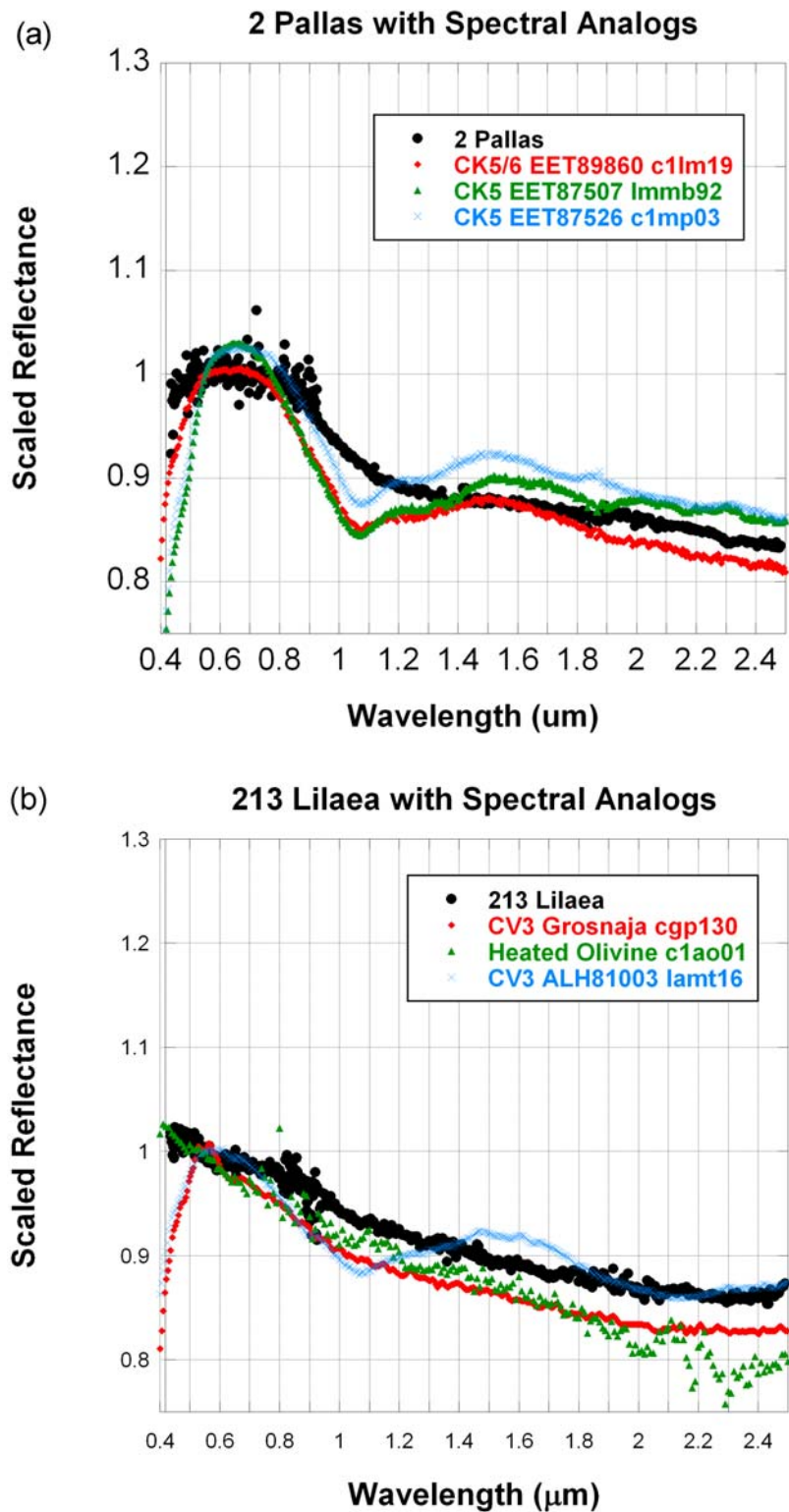


Figure 4. Meteorite spectral analogs for asteroids (a) 2 Pallas, (b) 213 Lillaea, (c) 1508 Kemi, and (d) 3200 Phaethon. Note the silicate band at $\sim 1.1 \mu\text{m}$ that is present in CK5 meteorites but absent in 2 Pallas. These meteorites represent the best (lowest χ^2) spectral and albedo matches found in the RELAB database. Note the extended Y-scale on the Phaethon plot. Phaethon is extremely blue.

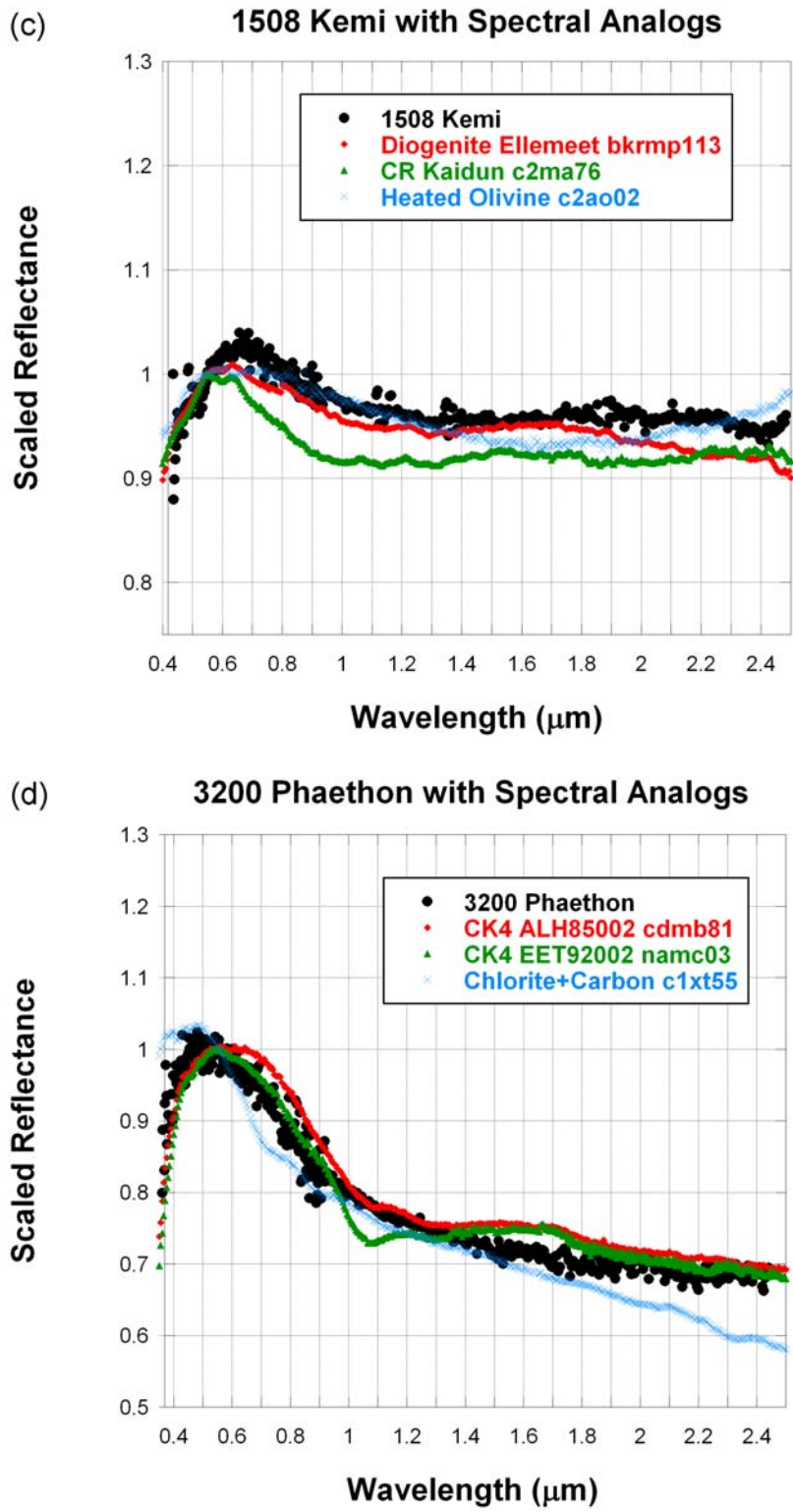


Figure 4. (continued)

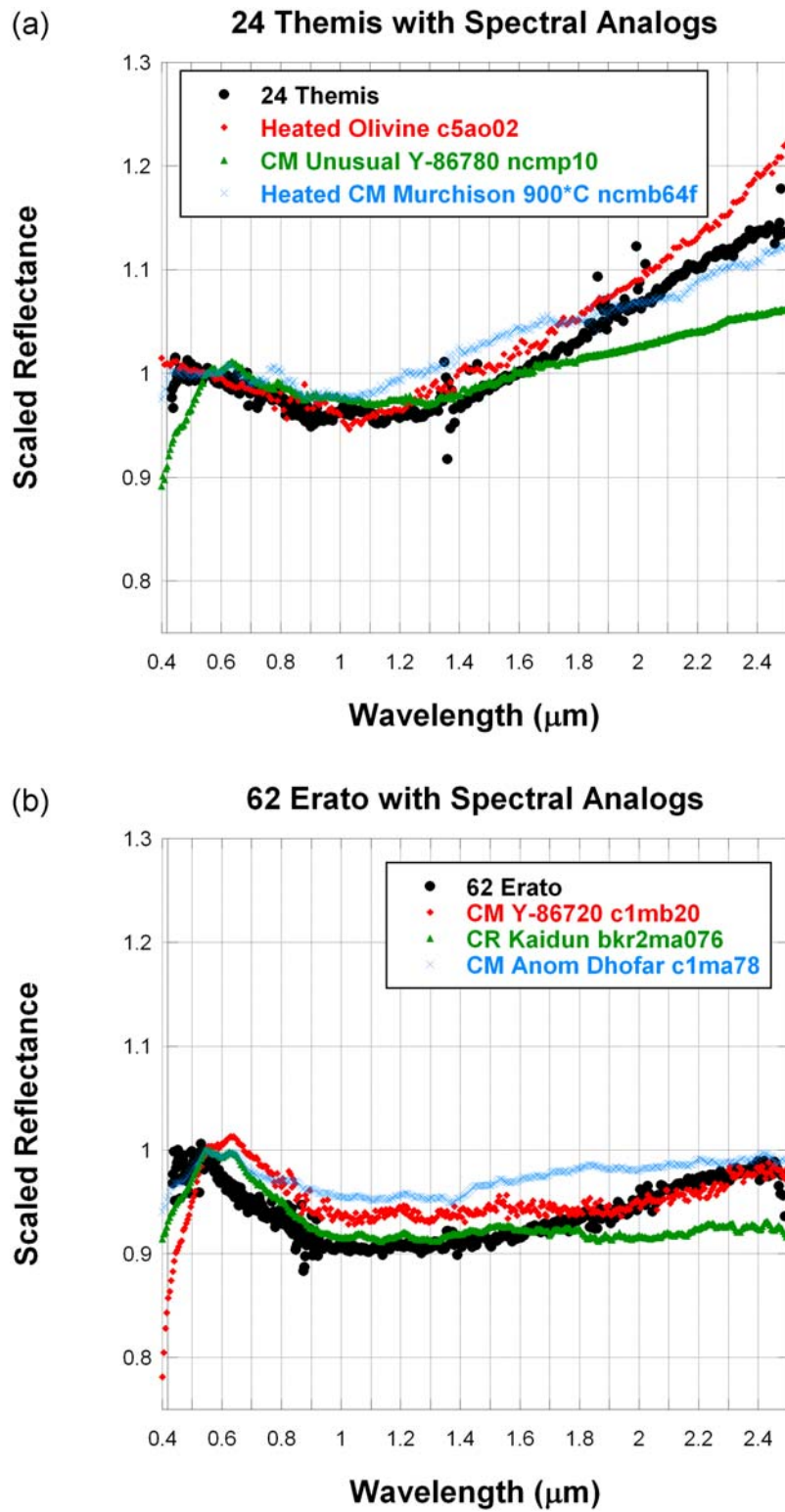


Figure 5. Meteorite spectral analogs for asteroids (a) 24 Themis, (b) 62 Erato, (c) 383 Janina, and (d) 431 Nephela.

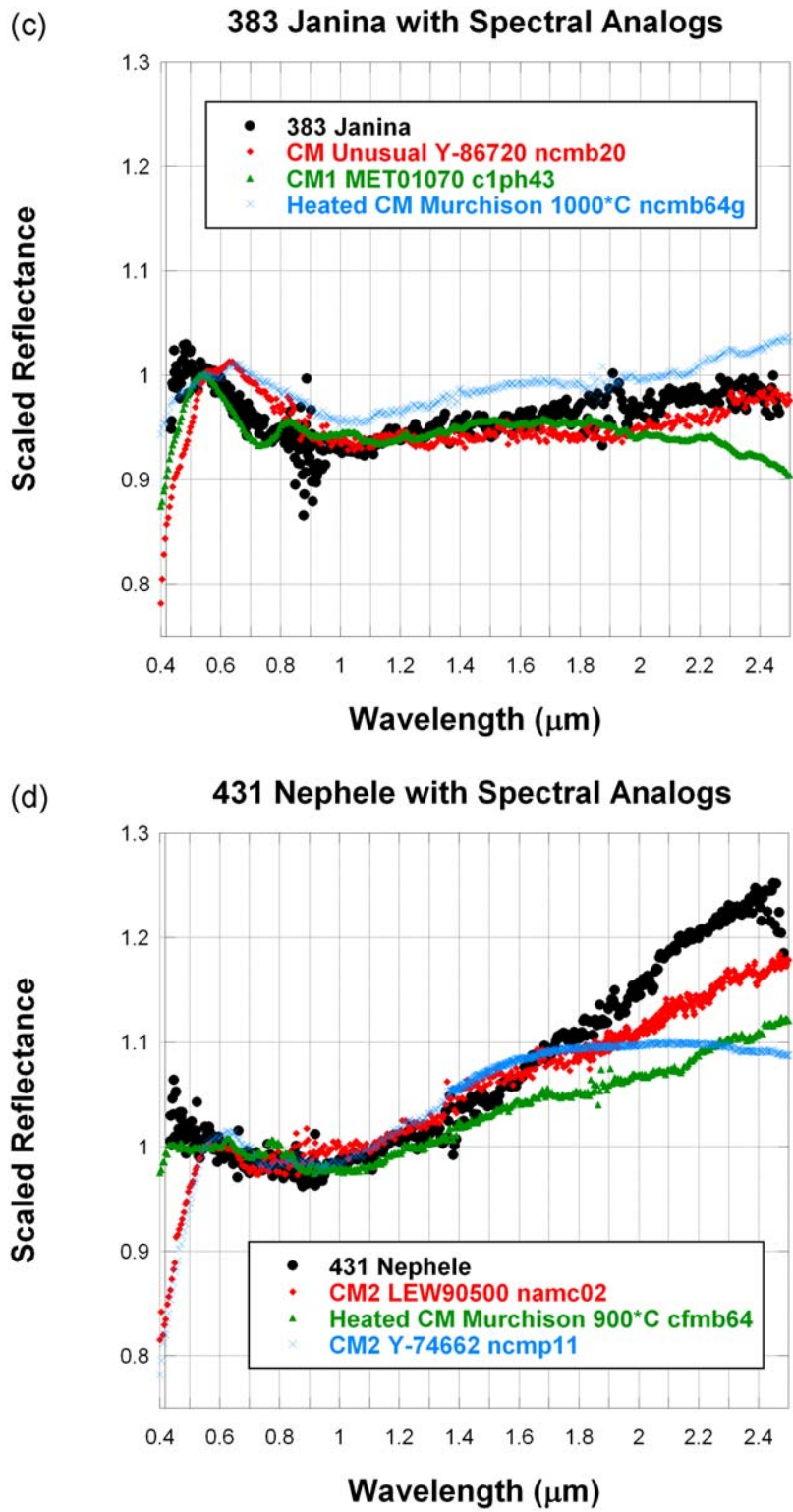


Figure 5. (continued)

Table 4. Dynamical Core of the Pallas Family

Asteroid Number	a (AU) ^a	e	$\text{Sin}(i)$	H_{mag} MPC
2	2.77092	0.28	0.55	3.93
531	2.78617	0.25	0.55	12.10
2382	2.75957	0.27	0.54	11.12
3579	2.73366	0.28	0.55	13.83
4969	2.75747	0.27	0.54	12.54
5222	2.77542	0.28	0.54	11.11
5234	2.76092	0.27	0.55	11.98
5330	2.76429	0.26	0.53	11.94
8009	2.77219	0.28	0.56	13.10
11064	2.75032	0.25	0.55	12.72
12377	2.76516	0.27	0.55	12.73
14916	2.73670	0.28	0.54	13.27
15834	2.77838	0.26	0.55	13.96
23830	2.78323	0.28	0.55	12.96
24793	2.71955	0.28	0.54	13.58
25853	2.77729	0.26	0.53	13.24
32773	2.77890	0.28	0.55	13.19
33166	2.78986	0.28	0.54	13.11
33750	2.79090	0.28	0.55	12.38
36273	2.76979	0.28	0.55	12.58
39646	2.75903	0.28	0.55	13.50
40101	2.73034	0.29	0.55	14.78
44232	2.76141	0.26	0.54	12.98
46037	2.75972	0.27	0.54	13.40
46536	2.78079	0.26	0.55	13.80
52229	2.75895	0.26	0.56	13.22
57050	2.76936	0.25	0.54	13.42
58296	2.72969	0.30	0.55	13.84
66714	2.72948	0.27	0.54	13.80
66803	2.77467	0.26	0.55	12.57
66846	2.75697	0.27	0.54	13.65
67370	2.71540	0.29	0.54	13.61
67779	2.72340	0.28	0.55	12.45
68299	2.73743	0.30	0.55	13.44
69371	2.73831	0.27	0.55	13.51
69931	2.75637	0.28	0.54	13.46
79086	2.77434	0.27	0.55	14.12
82899	2.73968	0.26	0.54	13.70
85483	2.72055	0.28	0.55	14.28
87006	2.78341	0.28	0.55	13.41
87306	2.75691	0.28	0.55	12.53
89662	2.72176	0.30	0.55	13.12
90212	2.73576	0.29	0.54	13.83
90368	2.74364	0.27	0.54	13.32
91399	2.77431	0.26	0.53	14.18
100590	2.77365	0.27	0.54	14.25
101283	2.77193	0.26	0.53	13.86
103779	2.75306	0.26	0.56	14.18
105061	2.72641	0.27	0.53	14.17
109640	2.77250	0.27	0.53	13.49
110323	2.72992	0.28	0.54	13.71
112876	2.71005	0.27	0.54	14.52
113770	2.75595	0.27	0.53	13.81
118223	2.77534	0.26	0.54	14.40
119368	2.71640	0.28	0.54	14.66
122277	2.76485	0.26	0.55	14.18
123349	2.76055	0.28	0.54	14.50
136038	2.75801	0.26	0.54	14.83
138406	2.70963	0.28	0.55	14.30
140951	2.73851	0.28	0.54	13.74
145861	2.77351	0.27	0.54	14.31
148027	2.79336	0.25	0.54	14.63
153652	2.77079	0.27	0.55	13.35
157914	2.79825	0.24	0.53	14.0
164196	2.71771	0.27	0.54	14.64
174441	2.71362	0.27	0.54	14.41
176413	2.77250	0.26	0.54	14.31

^aAU, arbitrary units; MPC, Minor Planet Center.

perhaps rescaling from 100 km does not work and/or it has an interior composition that differs from that assumed. (2) Small Pallas family members have been depleted by dynamical radiation effects over time. (3) Small Pallas family members have collisionally evolved over time and are thus now closer to Dohnanyi slope than they were originally.

Of note is an interesting similarity in the osculating orbits of 1508 and 6411:

a (AU) e ($^\circ$) i ($^\circ$)
 1508 Kemi 2.769 0.417 28.7
 6411 Tamaga 2.762 0.418 28.6
 For reference, Pallas has
 a (AU) e ($^\circ$) i ($^\circ$)
 2.77 0.23 34.8

[41] While dynamics have greatly changed the eccentricity and inclination of their orbits over time, numerical integrations show some evidence that 1508 and 6411 are peripheral parts of the Pallas family. We conclude that asteroids 2, 1508, and 6411 are dynamically related.

[42] Examining orbits, we also briefly checked to see whether any of the four asteroids in the Other group (229, 261, 505, 554) could be dynamically related to each other, to Pallas, or to Themis. The orbital elements of these objects are dissimilar and do not show any signs of potential dynamical relationship.

5. Discussion

[43] Our working hypothesis was that *Hiroi et al.* [1996] explained the composition of B-type asteroids. After several years of continued observation with higher-resolution instrumentation, has the Hiroi model held up to scrutiny? Our results suggest that yes, the Hiroi model still stands as a viable explanation of the observations, but only for the Themis group B types (for a refutation of the Hiroi model, see *Vilas and Sykes* [1996]). We find that 19 of 30 best fits in the Themis group were with heated CI or CM material, with Unusual CI or CM material (i.e., thermally metamorphosed CI or CM), or with heated olivine. We have found at least one such sample among the best three fits for all of the Themis group asteroids. This could mean that perhaps half of the Themis group is hydrated and half is not, or it could mean that the spectral data from 0.4 to 2.5 μm are ambiguous on the distinction between aqueous alteration versus thermal metamorphism. We find that the hypothesis of *Hiroi et al.* [1996] does not hold up for the Pallas group objects.

[44] If Themis group B types are composed of phyllosilicate-bearing carbonaceous chondrites, do they show hydration absorption features? Could this band be used as a “test” to resolve whether Themis group objects are hydrated? The 3 μm band has been detected on 24 Themis, 419 Aurelia, and 431 Nephele and has been marginally nondetected (ruled out) on 335 Goberta and 704 Interamnia (A. S. Rivkin et al., manuscript in preparation, 2010). *Vilas* [1994] found that $\sim 33\%$ of the 18 ECAS B-type asteroids tested positive for the detection of the 0.7 μm phyllosilicate feature. In Figure 8, we show a zoom plot of the 0.7 μm wavelength region, for a meteorite that shows the band, for an asteroid that shows the band, and for Themis. It is pretty clear that this spectrum of Themis does not show the band; however, *Fornasier et al.* [1999] showed a positive detection at the level of 4%, so the object may have some rotational

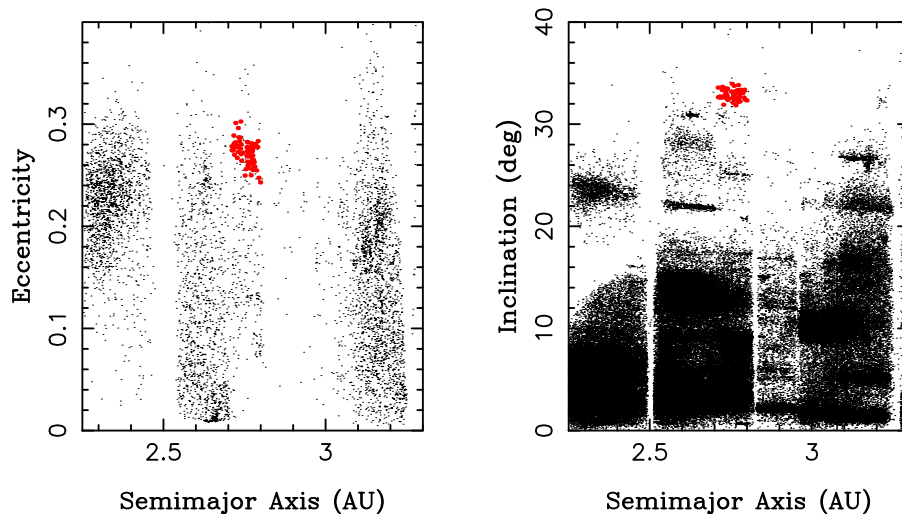


Figure 6. Orbital parameters of the Pallas family.

variations, but more observations are required. We suspect that 316 Goberta and 762 Pulcova may show evidence of the $0.7\ \mu\text{m}$ feature. Apparently, 67% of asteroids observed at both 0.7 and $3\ \mu\text{m}$ showed consistent bands indicating hydration [Howell *et al.*, 2001]. That means that 33% of objects observed do not. According to Rivkin *et al.* [2002], the $0.7\ \mu\text{m}$ band should not be present when the $3\ \mu\text{m}$ hydration band is absent. We quote Rivkin *et al.* [2002]: “a mild heating episode (occurring after the aqueous alteration), with temperatures reaching $400\text{--}600\ \text{°C}$, can explain the observations. Another possibility is that all the Fe^{2+} has been converted to Fe^{3+} , which would account for the $0.7\ \mu\text{m}$ band being absent on an object where the 3-micron band is seen.” So, the fact that the 0.7 and $3\ \mu\text{m}$ observations do not always agree is clearly indicating that something is missing in our understanding. We conclude that the evidence is yet too slim to draw conclusions about the hydration state of Themis group objects and also suggest that both hypotheses (aqueous alteration and thermal metamorphism) are currently consistent with our results. Certainly, future work should address this issue in the context of B-type asteroids.

[45] Rivkin *et al.* [2006] analyzed spectra of Ceres from 2.2 to $4.1\ \mu\text{m}$ and found evidence for carbonates and iron-rich clays, such as are found in CI meteorites. However, this compositional interpretation has not yet been resolved with the spectral evidence from 0.3 to $2.2\ \mu\text{m}$. To our knowledge, carbonates have not been detected on B types.

[46] What is the role of grain size in meteorite-asteroid spectral matches? Polarimetry data indicate that asteroid regoliths are dominated by grains on the order of $30\text{--}300\ \mu\text{m}$ in size, on average [Dollfus *et al.*, 1989]. The optical properties measured in the visible and near-infrared wavelengths will be dominated by the finest grain sizes, which tend to cling to and coat larger grains. In this work, we did not constrain grain size except to insist that a suggested match be of a particulate specimen. Most samples relevant to asteroid spectra have been obtained at grain sizes less than $300\ \mu\text{m}$; however, there is still room for a large amount of variety in reflectance properties of carbonaceous materials between 30 and $300\ \mu\text{m}$. Johnson and Fanale [1973]

showed the sense and magnitude of spectral variations that occur with grain size variations of the same sample for many different carbonaceous chondrite meteorites. In Figure 9, we show grain size separates of the CV3 meteorite Grosnaja. Immediately apparent is the large shift in brightness of the finer grain size ($<75\ \mu\text{m}$) relative to the coarser grain sizes ($75\text{--}500\ \mu\text{m}$). An albedo shift like this, from 6% to 12%, exceeds the threshold we placed on our brightness constraints in the analog search we conducted. This means that if an appropriate material did not exist at the right grain size for a match to our asteroid within the $\pm 3\text{--}5\%$ limits we set, then the material would be overlooked as a possible analog. We note also that the visible “blueing” trend observed (Figure 9, right) for coarser grains is consistent with the findings of Johnson and Fanale [1973]. Johnson and Fanale [1973] made their measurements using an integrating sphere, so illumination angle effects cannot be the cause of the blueing. Figure 9 illustrates one of the features of a spectrum library: the $<45\ \mu\text{m}$ grain size fraction is darker and bluer than the $<75\ \mu\text{m}$ grain size. This is contrary to what we would expect, that finer grain sizes are brighter and redder [Adams and Filice, 1967]. We suspect that particle

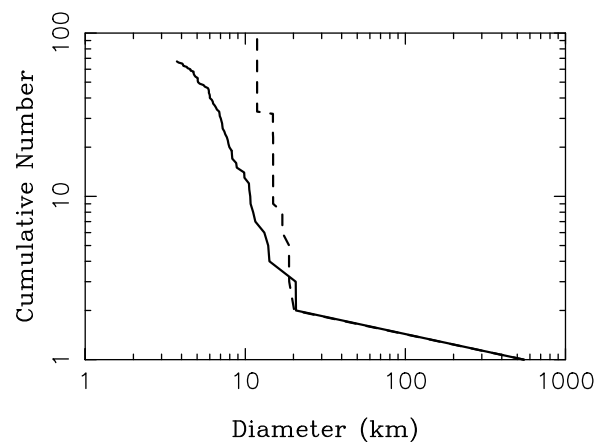


Figure 7. Size-frequency distribution of the Pallas family.

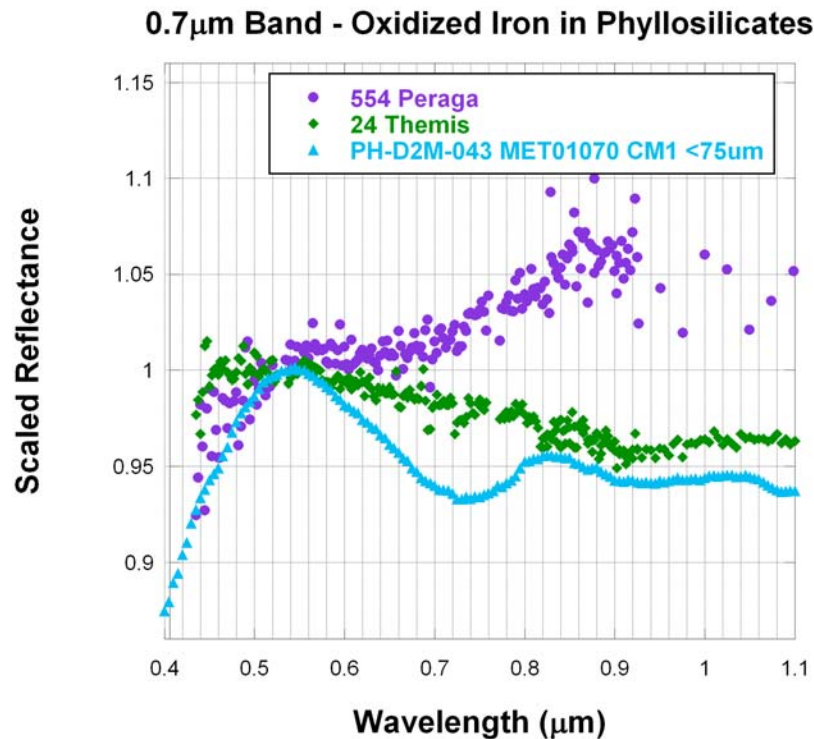


Figure 8. The $0.7 \mu\text{m}$ band, attributed to oxidized iron in phyllosilicate minerals, shows up strongly in this sample of the CM1 meteorite MET01070. The spectrum of 554 Peraga, a Bus-DeMeo Ch-type asteroid, is shown for comparison. In Peraga, we see how the $0.7 \mu\text{m}$ band manifests in many asteroid spectra. Asteroid 24 Themis does not show a band, consistent with thermal metamorphism of carbonaceous chondritic material and its match with CM Unusual meteorites.

compaction and/or sample cup filling methods differed between the two spectra, showing how important micro-physical properties can be to reflectance spectra. Because these small differences are not “resolved” to those who search a library database, we must take individual “matches” with a grain of salt and, rather, look for trends in groups of spectra, as we have attempted in the present work.

[47] What causes the negative slope that makes a B type a B type? We can begin to address this question using the evidence we have assembled here. Because the CV3 Grosnaja gets blue with coarser grain size [Johnson and Fanale, 1973; Gaffey, 1976; Shepard et al., 2008], our first suspicion was that the negative slope is caused by a particle size effect such that B types are somehow covered with coarser grains. Table 3 shows that the spectral evidence does not support this hypothesis. There is a slight tendency for coarser grain samples among the Pallas group matches (30% of matches contained particles coarser than $125 \mu\text{m}$ for the Pallas group, and 20% of matches contained particles coarser than $125 \mu\text{m}$ for the Themis group), but the differences are not strong enough to fully explain the phenomenon. Our next hypothesis was that hydrated species were to blame. However, we find most of the hydrated meteorite sample matches occurred for Themis group objects that have positive long-wavelength slopes, and very few hydrated samples showed up in the blue Pallas group. We conclude that, if anything, the opposite holds: the negative slope is due to nonhydrated carbonaceous chondrite meteorite materials,

measured at grain sizes appropriate for comparison to asteroid regoliths.

[48] What is the role of space weathering in all of this? Although we assume no role for the purposes of this project, we note that space-weathering effects may yet be shown to affect dark asteroids. Using statistical arguments, Lazzarin et al. [2006] showed that space weathering probably occurs on all asteroid types. Although this is true, many types lack the high-albedo and strong spectral band contrasts that make weathering effects easily detectable [Clark et al., 2002]. It is known that opaque materials mask the optical effects of space-weathering products [Pieters et al., 2000]. Space-weathering simulation experiments with low-albedo enstatite chondrites, for example, suggest that alteration of these meteorites produces very little spectral variation [Vernazza et al., 2009]. Some workers suggest that carbon-rich surfaces alter to become spectrally red [Lazzarin et al., 2006], and others have found evidence that spectral redness decreases [Nesvornyy et al., 2005; Hiroi et al., 2004]. Irradiation experiments with hydrocarbon materials performed by Moroz et al. [2004] resulted in progressive reduction of steep positive spectral slopes and a moderate increase in reflectance in the visible range. These workers attribute the optical changes to progressive carbonization of the target materials. Rivkin et al. [2002] make note of an important fact about weathering: “while nanophase Fe has a lower albedo than olivine and pyroxene, and small amounts can radically change a spectrum, it (nanophase iron) has a higher albedo than the opaque

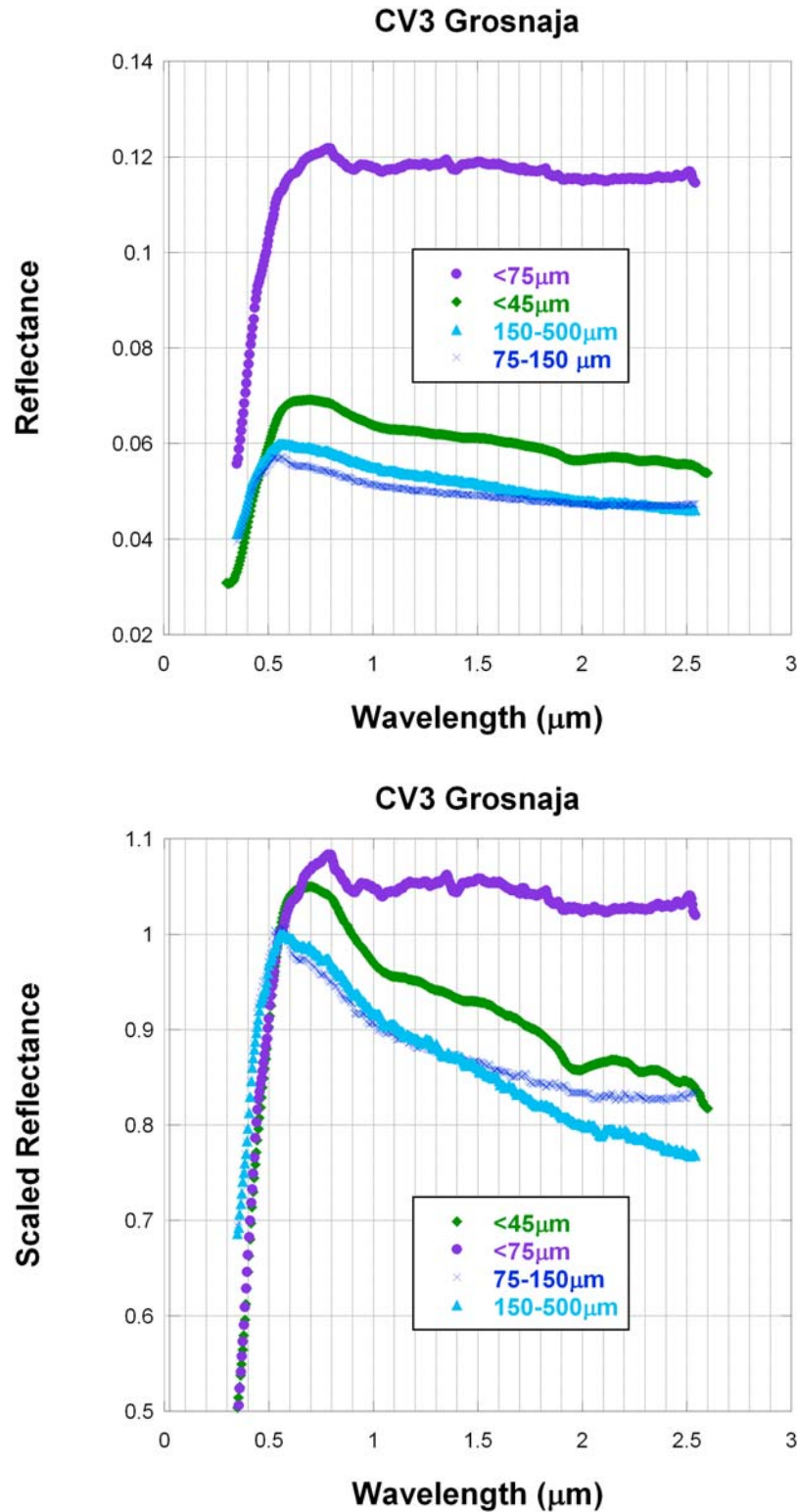


Figure 9. The grain size effect is illustrated by these particle size separates of the meteorite Grosnaja, a CV3 chondrite. (left) Spectra are shown in relative reflectance. Note the large variation in brightness at $0.55 \mu\text{m}$ that can occur with particle comminution, as described by *Johnson and Fanale* [1973]. (right) Spectra are shown normalized to 1.0 at $0.55 \mu\text{m}$.

minerals present.” We know that for brighter minerals, nanophase Fe darkens and flattens a spectrum. It follows that for darker minerals, nanophase Fe may brighten and flatten a spectrum. Indeed, we note that 3200 Phaethon and 2 Pallas could represent this weathering sequence. It is possible that the two objects are compositionally similar and that Phaethon represents a freshly exposed surface while Pallas represents a highly space-weathered surface. Since there is no consensus at this point, we must await possible future discoveries from space-weathering simulations, experiments, and laboratory study following a sample return spacecraft mission.

[49] *Belskaya et al.* [2005] found that (Tholen) F-type asteroids are distinct from other low-albedo objects, having much lower polarization inversion angles ($\sim 14\text{--}16^\circ$ as opposed to $19.5\text{--}21.5^\circ$ for P, C, G, and B classes). In particular, 419 Aurelia, with an inversion angle of 14° and a $P_{\min} = 1\%$, is the first asteroid for which a saturation effect of the negative polarization was found. This effect is the constancy of both the minimum of polarization and inversion angle when the surface albedo of asteroids decreases (albedo of ~ 0.06) and was previously found in laboratory simulation studies for very dark samples prepared as various mixtures of carbon soot and silicates [*Zellner et al.*, 1977; *Shkuratov et al.*, 1992]. *Belskaya et al.* [2005] interpreted the small values of the parameters P_{\min} and inversion angle for F-type asteroids as a diagnostic of optical homogeneity of the regolith microstructure on scales of the order of the wavelength. In the study by *Belskaya et al.* [2005], this interpretation was considered “consistent with the fact that these asteroids have flat spectra, as any spectral feature (bands or UV absorption) is largely produced by relatively bright regolith components that should also strengthen the negative polarization. One of the feasible mechanisms that could contribute to surface optical homogeneity is carbon deposits on upper layer particles of the asteroid regolith. The deposits might result from pyrolysis of carbon-bearing (organic) matter” that has suffered space weathering [see *Belskaya et al.*, 2005, and references therein].

[50] The Tholen taxonomy uses albedo as a major factor in asteroid class designation. In contrast, the Bus and Binzel (visible wavelength) taxonomic system, and the subsequent Bus-DeMeo (vis-near-infrared) system, do not use albedo. These later systems also use different wavelength ranges and therefore do not replace Tholen. Rather, they can be used in parallel with the Tholen system. The question is, Do the original Tholen B/F designations predict the behavior of near-infrared spectra? According to our results, there is no evidence that the Tholen B/F designation is correlated with the eventual Bus-DeMeo designation. Among our Pallas group, we have two B, four F, and one C Tholen class. Among our Themis group, we have five B, four F, and one C Tholen class. Contrast that with the Bus-DeMeo classifications of all B types for the Pallas group and mostly C types for the Themis group. Because the Tholen taxonomy distinguished between B and F types on the basis of the UV feature, it is not surprising that these later studies (that do not resolve the UV feature) do not depend on the UV feature.

6. Conclusion

[51] We combine new observations of 13 objects with published observations of 9 objects to assemble a total of 22

B-type spectra. Our targets are composed of anything that anyone has ever called a B type. We have found that the assembled spectra fall into three groups based on spectral shape (Pallas, Themis, and Other). We have compared these spectra with 15,000 laboratory spectra of meteorites and minerals. This study allowed various grain-size ranges and separates and constrained relative brightnesses of the asteroids and the meteorites to be similar. We find that, allowing for uncertainties caused by (1) grain sizes of asteroid surfaces and (2) disparate measurements of albedo and reflectance, we can find satisfactory spectral matches for most of the asteroids in our sample. Our results for Themis group objects are consistent with previous work. We confirm the suggestions of others [*Gaffey and McCord*, 1978; *Vilas et al.*, 1994; *Hiroi et al.*, 1996] that C-type asteroids are consistent with CM, CI, and CM/CI Unusual (thermally metamorphosed) carbonaceous chondrites. Our results for Pallas group objects are not consistent with previous work. We find that most Pallas group objects can be matched with CK, CO, or CV meteorites. We suggest that the negative slope (from ~ 0.5 to $\sim 1.1 \mu\text{m}$ and beyond) of B types can be attributed to CK-, CO-, and CV-type mineralogies. Interestingly, we find that the differences in spectral properties between 3200 Phaethon and 2 Pallas can be explained by space weathering of a common starting composition if space weathering of low-albedo materials results in brightening and flattening of the spectra from ~ 0.5 to $2.5 \mu\text{m}$.

7. Future Work

[52] This work has revealed a few interesting lines of investigation for future work. (1) If the groupings, meteorite matches, and hydration states that we have found are real, then $3 \mu\text{m}$ spectra that can detect the presence and relative abundance of phyllosilicates should be consistent. (2) More Pallas family observations would help to understand the composition and origin of the Pallas group we have described. (3) A comprehensive parametric description of the RELAB database of meteorite spectra that accounts for grain size, meteorite class, and petrologic grades would be helpful in forming meteorite-asteroid links. (4) It would be interesting to examine the Sloan Digital Sky Survey colors for Pallas and Themis families. (5) An understanding of the statistical significance of a match between an asteroid and a meteorite spectrum should be developed to help us determine the probability that a piece of a given asteroid exists in our Earthly collection. (6) It would be helpful to have more laboratory simulations of space weathering of low-albedo materials accompanied by retrieval of surface samples of an asteroid.

[53] **Acknowledgments.** B.E.C. thanks the Observatory of Paris for its kind hospitality. The Bus-DeMeo Taxonomy Classification is from the Web tool by S. L. Slivan, developed at MIT with the support of NSF grant 0506716 and NASA grant NAG5-12355. We thank Irina Belskaya and Rosario Brunetto for very helpful conversations and Faith Vilas for providing a helpful review. Bobby Bus was instrumental in the early phases of the data reduction and was a member of the team contributing spectra of asteroids 2, 1508, 3200, and 6411. We also acknowledge the excellent telescope operation of Bill Golisch and Paul Sears. This work uses spectra from the NASA RELAB facility at Brown University. J.L. gratefully acknowledges support from the Spanish “Ministerio de Ciencia e Innovación” project AYA2008-06202-C03-02. B.E.C. and R.P.B. were guest astronomers at the Observatoire de Paris. B.E.C., J.Z., H.C., A.S.R., R.P.B., M.E.O. - B., J.L., and T.M. -D. were guest observers at the NASA Infrared Tele-

spectroscopy Facility. H.C. was a guest astronomer at the Observatoire de la Côte d'Azur. RPB is a Chercheur Associé at the Observatoire de Paris.

References

- Adams, J., and A. Filice (1967), Spectral reflectance 0.4 to 2.0 microns of silicate rock powders, *J. Geophys. Res.*, **72**, 5705–5715, doi:10.1029/JZ072i022p05705.
- Bell, J. F., B. R. Hawke, P. D. Owensby, and M. J. Gaffey (1988), The 52-color asteroid survey, final results and interpretations, *Proc. Lunar Planet. Sci. Conf., XIXth*, 57–58.
- Bell, J. F., D. Davis, W. K. Hartmann, and M. J. Gaffey (1989), Asteroids: The big picture, in *Asteroids II*, edited by R. P. Binzel, T. Gehrels, and M. S. Matthews, pp. 921–948, Univ. of Ariz. Press, Tucson.
- Belskaya, I., et al. (2005), The F-type asteroids with small inversion angles of polarization, *Icarus*, **178**, 213–221, doi:10.1016/j.icarus.2005.04.015.
- Belskaya, I. N., A.-C. Levasseur-Regourd, A. Cellino, Y. S. Efimov, N. M. Shakhovskoy, E. Hadamcik, and P. Bendjoya (2009), Polarimetry of main belt asteroids: Wavelength dependence, *Icarus*, **199**, 97–105.
- Burbine, T., T. McCoy, A. Meibom, B. Gladman, and K. Keil (2002), Meteorite parent bodies: Their number and identification, in *Asteroids III*, edited by W. F. Bottke Jr., A. Cellino, P. Paolicchi, and R. P. Binzel, pp. 653–667, Univ. of Ariz. Press, Tucson.
- Bus, S. J., and R. P. Binzel (2002a), Phase II of the Small Main-Belt Asteroid Spectroscopic Survey: The observations, *Icarus*, **158**, 106–145, doi:10.1006/icar.2002.6857.
- Bus, S. J., and R. P. Binzel (2002b), Phase II of the Small Main-Belt Asteroid Spectroscopic Survey: A feature-based taxonomy, *Icarus*, **158**, 146–177, doi:10.1006/icar.2002.6856.
- Bus, S. J., R. P. Binzel, and E. Volquardsen (2003), Characterizing the visible and near-IR spectra of asteroids using principal component analysis, *Bull. Am. Astron. Soc.*, **35**, 976.
- Bus, S. J., F. E. DeMeo, R. P. Binzel, and S. M. Slivan (2008), Bus-DeMeo taxonomy: Extending asteroid taxonomy into the near-infrared, *Bull. Am. Astron. Soc.*, **40**, 42, Abstract 28.22.
- Campins, H., K. Hargrove, E. S. Howell, M. S. Kelley, J. Licandro, T. Mothé-Diniz, J. Ziffer, and Y. Fernandez (2009), Confirming water ice on the surface of asteroid 24 Themis, *Bull. Am. Astron. Soc.*, **41**, 22.
- Chapman, C. R., and M. Gaffey (1979), Reflectance spectra for 277 asteroids, in *Asteroids*, edited by T. Gehrels and M. S. Matthews, pp. 655–687, Univ. of Ariz. Press, Tucson.
- Clark, B. E., et al. (2001), Space weathering on Eros: Constraints from albedo and spectral measurements of Psyche crater, *Meteorit. Planet. Sci.*, **36**, 1617–1638, doi:10.1111/j.1945-5100.2001.tb01853.x.
- Clark, B. E., B. Hapke, C. Pieters, and D. Britt (2002), Asteroid space weathering and regolith evolution, in *Asteroids III*, edited by W. F. Bottke Jr., A. Cellino, P. Paolicchi, and R. P. Binzel, pp. 585–599, Univ. of Ariz. Press, Tucson.
- Clark, B. E., M. E. Ockert-Bell, E. A. Cloutis, D. Nesvorný, T. Mothé-Diniz, and S. J. Bus (2009), Spectroscopy of K-complex asteroids: Parent bodies of carbonaceous meteorites? *Icarus*, **202**, 119–133, doi:10.1016/j.icarus.2009.02.027.
- Consolmagno, G. J., and M. J. Drake (1977), Composition and evolution of the eucrite parent body: Evidence from rare earth elements, *Geochim. Cosmochim. Acta*, **41**, 1271–1282, doi:10.1016/0016-7037(77)90072-2.
- Delbó, M., A. dell'Oro, A. W. Harris, S. Mottola, and M. Mueller (2007), Thermal inertia of near-Earth asteroids and implications for the magnitude of the Yarkovsky effect, *Icarus*, **190**, 236–249, doi:10.1016/j.icarus.2007.03.007.
- DeMeo, F. E., R. P. Binzel, S. M. Slivan, and S. J. Bus (2009), An extension of the Bus asteroid taxonomy into the near-infrared, *Icarus*, **202**, 160–180, doi:10.1016/j.icarus.2009.02.005.
- Dollfus, A., M. Wolff, J. E. Geake, D. F. Lupishko, and L. M. Dougherty (1989), Photopolarimetry of asteroids, in *Asteroids II*, edited by R. P. Binzel, T. Gehrels, and M. S. Matthews, pp. 594–616, Univ. of Ariz. Press, Tucson.
- Durda, D., W. Bottke, D. Nesvorný, B. Enke, W. Merline, E. Asphaug, and D. Richardson (2007), Size-frequency distributions of fragments from SPH/N-body simulations of asteroid impacts: Comparison with observed asteroid families, *Icarus*, **186**, 498–516, doi:10.1016/j.icarus.2006.09.013.
- Fanale, F., B. E. Clark, and J. F. Bell (1992), A spectral analysis of ordinary chondrites, S-type asteroids, and their component minerals, *J. Geophys. Res.*, **97**, 20,863–20,874, doi:10.1029/92JE02228.
- Feierberg, M. A., L. A. Lebofsky, and D. J. Tholen (1985), The nature of C-class asteroids from 3 μ m spectrophotometry, *Icarus*, **63**, 183–191, doi:10.1016/0019-1035(85)90002-8.
- Fornasier, S., M. Lazzarin, C. Barbieri, and M. A. Barucci (1999), Spectroscopic comparison of aqueous altered asteroids with CM2 carbonaceous chondrite meteorites, *Astron. Astrophys.*, **135**, 65–73.
- Fornasier, S., I. Belskaya, Y. Shkuratov, C. Percheche, C. Barbieri, E. Giro, and H. Navasardyan (2006), Polarimetric survey of asteroids with the Asiago telescope, *Astron. Astrophys.*, **455**, 371–377, doi:10.1051/0004-6361:20064836.
- Gaffey, M. J. (1976), Spectral reflectance characteristics of the meteorite classes, *J. Geophys. Res.*, **81**, 905–920, doi:10.1029/JB081i005p0905.
- Gaffey, M. J., and T. McCord (1978), Asteroid surface materials: Mineralogical characterization from reflectance spectra, *Space Sci. Rev.*, **21**, 555–628, doi:10.1007/BF00240908.
- Gaffey, M. J., T. H. Burbine, J. L. Piatek, K. L. Reed, D. A. Chaky, J. F. Bell, and R. H. Brown (1993), Mineralogical variations within the S-type asteroid class, *Icarus*, **106**, 573–602, doi:10.1006/icar.1993.1194.
- Gaffey, M. J., E. Cloutis, M. S. Kelley, and K. L. Reed (2002), Mineralogy of asteroids, in *Asteroids III*, edited by W. F. Bottke Jr., A. Cellino, P. Paolicchi, and R. P. Binzel, pp. 183–204, Univ. of Ariz. Press, Tucson.
- Hiroi, T., C. M. Pieters, M. E. Zolensky, and M. E. Lipschutz (1993), Evidence of thermal metamorphism on the C, G, B, and F asteroids, *Science*, **261**, 1016–1018, doi:10.1126/science.261.5124.1016.
- Hiroi, T., M. E. Zolensky, C. Pieters, and M. Lipschutz (1996), Thermal metamorphism of the C, G, B, and F asteroids seen from the 0.7 micron, 3 micron, and UV absorption strengths in comparison with carbonaceous chondrites, *Meteorit. Planet. Sci.*, **31**, 321–327.
- Hiroi, T., C. M. Pieters, M. J. Rutherford, M. E. Zolensky, S. Sasaki, Y. Ueda, and M. Miyamoto (2004), What are the P-type asteroids made of? [CD-ROM] *Lunar Planet. Sci.*, XXXV.
- Howell, E., A. Rivkin, F. Vilas, and A. M. Soderberg (2001), Aqueous alteration in low albedo asteroids, *Lunar Planet. Sci.* [CD-ROM], XXXII, Abstract 2058.
- Hsieh, H., and D. Jewitt (2006), A population of comets in the main asteroid belt, *Science*, **312**, 561–563, doi:10.1126/science.1125150.
- Jenniskens, P., et al. (2009), The impact and recovery of asteroid 2008 TC3, *Nature*, **458**, 485–488, doi:10.1038/nature07920.
- Johnson, T. V., and F. Fanale (1973), Optical properties of carbonaceous chondrites and their relationship to asteroids, *J. Geophys. Res.*, **78**, 8507–8518, doi:10.1029/JB078i035p08507.
- Jones, T. D., L. A. Lebofsky, J. S. Lewis, and M. S. Marley (1990), The composition of the C, P, and D asteroids: Water as a tracer of thermal evolution in the outer belt, *Icarus*, **88**, 172–192, doi:10.1016/0019-1035(90)90184-B.
- Lazzarin, M., S. Fornasier, M. A. Barucci, and C. Barbieri (2001), Low resolution spectroscopic survey of main belt asteroids: looking for aqueous alteration products, paper presented at Asteroids 2001: From Piazzini to the 3rd Millennium, Osservatorio Astronomico “G. S. Vaiana” di Palermo, Palermo, Italy, 11–16 June.
- Lazzarin, M., S. Marchi, L. Moroz, R. Brunetto, S. Magrin, and P. Paolicchi (2006), Space weathering in the main asteroid belt: The big picture, *Astrophys. J.*, **647L179** doi:10.1086/507448.
- Lazzaro, D., C. A. Angeli, J. M. Carvano, T. Mothé-Diniz, R. Duffard, and M. Florczak (2004), S³OS²: The visible spectroscopic survey of 820 asteroids, *Icarus*, **172**, 179–220.
- Licandro, J., H. Campins, T. Mothé-Diniz, N. Pinilla-Alonso, and J. de León (2007), The nature of comet-asteroid transition object (3200) Phaethon, *Astron. Astrophys.*, **461751757** doi:10.1051/0004-6361:20065833.
- Lord, S. (1992), A new software tool for computing Earth's atmospheric transmission of near- and far-infrared radiation, *Tech. Memo.* 103957, NASA, Greenbelt, Md.
- Marzari, F., D. Davis, and V. Vanzani (1995), Collisional evolution of asteroid families, *Icarus*, **113**, 168–187, doi:10.1006/icar.1995.1014.
- Moroz, L., G. Baratta, G. Strazzulla, L. Starukhina, E. Dotto, M. A. Barucci, G. Arnold, and E. Distefano (2004), Optical alteration of complex organics induced by ion irradiation: 1. Laboratory experiments suggest unusual space weathering trend, *Icarus*, **170**, 214, doi:10.1016/j.icarus.2004.02.003.
- Mothé-Diniz, T., F. Roig, and J. M. Carvano (2005), Reanalysis of asteroid families structure through visible spectroscopy, *Icarus*, **174**, 54–80, doi:10.1016/j.icarus.2004.10.002.
- Mothé-Diniz, T., J. M. Carvano, S. J. Bus, R. Duffard, and T. H. Burbine (2008), Mineralogical analysis of the Eos family from near-infrared spectra, *Icarus*, **195**, 277–294, doi:10.1016/j.icarus.2007.12.005.
- Nesvorný, D., R. Jedicke, R. Whiteley, and Z. Ivezić (2005), Evidence for asteroid space weathering from the Sloan Digital Sky Survey, *Icarus*, **173**, 132–152, doi:10.1016/j.icarus.2004.07.026.
- Nesvorný, D. R., W. Bottke, D. Vokrouhlický, M. Sykes, D. J. Lien, and J. Stansberry (2008), Origin of the near-ecliptic circumsolar dust band, *Astrophys. J.*, **679**, L143–L146, doi:10.1086/588841.
- Ockert-Bell, M., B. E. Clark, M. K. Shepard, A. Rivkin, R. Binzel, C. Thomas, F. E. DeMeo, S. J. Bus, and S. Shah (2008), Observations of X/M-

- asteroids across multiple wavelengths, *Icarus*, *195*, 206–219, doi:10.1016/j.icarus.2007.11.006.
- Ostrowski, D. R., D. W. G. Sears, K. M. Gietzen, and C. H. S. Lacy (2009), An investigation of phyllosilicates, C chondrites, and C asteroids using continuum slopes of near infrared spectra, *Proc. Lunar Planet. Sci. Conf., XLth*, Abstract 1136.
- Pieters, C. (1983), Strength of mineral absorption features in the transmitted component of near-infrared reflected light: First results from RELAB, *J. Geophys. Res.*, *88*, 9534–9544, doi:10.1029/JB088iB11p09534.
- Pieters, C. M., L. Taylor, S. Noble, L. Keller, B. Hapke, R. Morris, C. Allen, D. McKay, and S. Wentworth (2000), Space weathering on airless bodies: Resolving a mystery with lunar samples, *Meteorit. Planet. Sci.*, *35*, 1101–1107, doi:10.1111/j.1945-5100.2000.tb01496.x.
- Rayner, J. T., D. Toomey, P. Onaka, A. Denault, W. Stahlberger, W. Vacca, and M. Cushing (2003), SpeX: A medium-resolution 0.8–5.5 μm spectrograph and imager for the NASA Infrared Telescope Facility, *Publ. Astron. Soc. Pac.*, *115*(805), 362–382, doi:10.1086/367745.
- Rivkin, A. S., and J. P. Emery (2008), Water ice on 24 Themis?, paper presented at 10th Asteroids, Comets, Meteors Conference, Johns Hopkins Univ. Appl. Physics Lab., Baltimore, Md.
- Rivkin, A. S., E. S. Howell, F. Vilas, and L. A. Lebofsky (2002), Hydrated minerals on asteroids: The astronomical record, in *Asteroids III*, edited by W. F. Bottke Jr., A. Cellino, P. Paolicchi, and R. P. Binzel, pp. 235–253, Univ. of Ariz. Press, Tucson.
- Rivkin, A. S., E. Volquarsden, and B. E. Clark (2006), The surface composition of Ceres: Discovery of carbonates and iron-rich clays, *Icarus*, *185*, 563–567, doi:10.1016/j.icarus.2006.08.022.
- Shepard, M., et al. (2008), Multi-wavelength observations of Asteroid 2100 Ra-Shalom, *Icarus*, *193*, 20–38, doi:10.1016/j.icarus.2007.09.006.
- Shkuratov, Y. G., N. V. Opanasenko, and M. A. Kreslavsky (1992), Polarimetric and photometric properties of the Moon: Telescope observation and laboratory simulation. 1. The negative polarization, *Icarus*, *95*, 283–299, doi:10.1016/0019-1035(92)90044-8.
- Sunshine, J. M., S. J. Shelte, T. J. McCoy, T. H. Burbine, C. M. Corrigan, and R. P. Binzel (2004), High-calcium pyroxene as an indicator of igneous differentiation in asteroids and meteorites, *Meteorit. Planet. Sci.*, *39*, 1343–1357, doi:10.1111/j.1945-5100.2004.tb00950.x.
- Tedesco, E. F., P. V. Noah, M. Moah, and S. D. Price (2002), The supplemental IRAS minor planet survey, *Astron. J.*, *123*, 10,565–10,585.
- Tholen, D. J. (1984), Asteroid taxonomy from cluster analysis of photometry, Ph.D. dissertation, Univ. of Ariz., Tucson.
- Tholen, D. J., and M. A. Barucci (1989), Asteroid taxonomy, in *Asteroids II*, edited by R. P. Binzel et al., pp. 298–315, Univ. of Ariz. Press, Tucson, Arizona.
- Vernazza, P., R. Brunetto, R. Binzel, C. Perron, D. Fulvio, G. Strazzulla, and M. Fulchignoni (2009), Plausible parent bodies for enstatite chondrites and mesosiderites: Implications for Lutetia's fly by, *Icarus*, *202*, 477–486, doi:10.1016/j.icarus.2009.03.016.
- Vilas, F. (1994), A cheaper, faster, better way to detect water of hydration on solar system bodies, *Icarus*, *111*, 456–467, doi:10.1006/icar.1994.1156.
- Vilas, F., and M. J. Gaffey (1989), Phyllosilicate absorption features in main-belt and outer-belt asteroid reflectance spectra, *Science*, *246*, 790–792, doi:10.1126/science.246.4931.790.
- Vilas, F., and M. Sykes (1996), Are low-albedo asteroids thermally metamorphosed? *Icarus*, *124*, 483–489, doi:10.1006/icar.1996.0224.
- Vilas, F., S. M. Larson, E. C. Hatch, and K. S. Jarvis (1993), CCD reflectance spectra of selected asteroids II: Low albedo asteroid spectra and data extraction techniques, *Icarus*, *105*, 67–78, doi:10.1006/icar.1993.1111.
- Vilas, F., K. S. Jarvis, and M. J. Gaffey (1994), Iron alteration minerals in the visible and near-infrared spectra of low-albedo asteroids, *Icarus*, *109*, 274–283, doi:10.1006/icar.1994.1093.
- Yanai, K., and H. Kojima (1995), *Catalog of the Antarctic Meteorites*, 230 pp., Natl. Inst. Polar Res., Tokyo.
- Zellner, B., M. Leake, T. LeBertre, M. Duseaux, and A. Dollfus (1977), The asteroid albedo scale. I. Laboratory polarimetry of meteorites, *Proc. Lunar Sci. Conf., VIIIth*, 1091–1110.
- Zellner, B., D. J. Tholen, and E. F. Tedesco (1985), The eight color asteroid survey: Results for 589 minor planets, *Icarus*, *61*, 355–416, doi:10.1016/0019-1035(85)90133-2.
- Ziffer, J., H. Campins, E. S. Howell, J. Licandro, M. Walker, R. Deshpande, and K. Hargrove (2008), Evidence for space weathering in the near-infrared spectra of primitive asteroids, *Bull. Am. Astron. Soc.*, *40*, 509.
- Zolensky, M. E., A. V. C. Ivanov, S. V. Yang, D. W. Mittlefehldt, and K. Ohsumi (1996), The Kaidun meteorite: Mineralogy of an unusual CM lithology, *Meteorit. Planet. Sci.*, *31*, 484–493.

M. A. Barucci, F. DeMeo, S. Fornasier, and M. Fulchignoni, Laboratoire d'Etudes Spatiales et d'Instrumentation en Astrophysique, Observatoire de Paris, 5 Place Jules Jansen, 92190 Meudon, France.

R. P. Binzel, Department of Earth, Atmospheric and Planetary Sciences, Massachusetts Institute of Technology, Cambridge, MA 02139, USA.

H. Campins, Department of Physics, University of Central Florida, Orlando, FL 32816, USA.

B. E. Clark and M. E. Ockert-Bell, Department of Physics, Ithaca College, 953 Danby Road, Ithaca, NY 14853, USA. (bclark@ithaca.edu)

T. Hiroi, Brown University, Department of Geological Sciences, Providence, RI 02912, USA.

J. Licandro, Instituto de Astrofísica de Canarias, Via L'actea s/n, 38200 La Laguna, Tenerife, Spain.

T. Mothé-Diniz, Universidade Federal do Rio de Janeiro, Observatório do Valongo, Ladeira Pedro Antônio, 43 CEP 20080-090, Rio de Janeiro, Brazil.

D. Nesvorný, Department of Space Studies, Southwest Research Institute, Boulder, CO 80302, USA.

A. S. Rivkin, Applied Physics Laboratory, Johns Hopkins University, Laurel, MD 20723, USA.

J. Ziffer, Department of Physics, University of Southern Maine, Portland, ME 04104, USA.